JACS
JOURNAL OF THE AMERICAN CHEMICAL SOCIETY
Article
pubs.acs.org/JACS

Photolytic Generation of Benzhydryl Cations and Radicals from Quaternary Phosphonium Salts: How Highly Reactive Carbocations Survive Their First Nanoseconds

Johannes Ammer,[†] Christian F. Sailer,[‡] Eberhard Riedle,[‡] and Herbert Mayr*,[†]

[†]Department Chemie, Ludwig-Maximilians-Universität München, Butenandtstrasse 5-13 (Haus F), 81377 München, Germany
[‡]Lehrstuhl für BioMolekulare Optik, Ludwig-Maximilians-Universität München, Oettingenstrasse 67, 80538 München, Germany

Supporting Information

ABSTRACT: UV irradiation (266 or 280 nm) of benzhydryl triarylphosphonium salts $Ar_2CH\text{-}PAr_3^+X^-$ yields benzhydryl cations Ar_2CH^+ and/or benzhydryl radicals $Ar_2CH^\bullet$. The efficiency and mechanism of the photo-cleavage were studied by nanosecond laser flash photolysis and by ultrafast spectroscopy with a state-of-the-art femtosecond transient spectrometer. The influences of the photo-electrofuge (Ar_2CH^+), the photo-nucleofuge (PPh_3 or $P(p\text{-Cl-}C_6H_4)_3$), the counterion ($X^- = BF_4^-$, SbF_6^-, Cl^-, or Br^-), and the solvent (CH_2Cl_2 or CH_3CN) were investigated. Photogeneration of carbocations from $Ar_2CH\text{-}PAr_3^+BF_4^-$ or $\text{-}SbF_6^-$ is considerably more efficient than from typical neutral precursors (e.g., benzhydryl chlorides or bromides). The photochemistry of phosphonium salts is controlled by the degree of ion pairing, which depends on the solvent and the concentration of the phosphonium salts. High yields of carbocations are obtained by photolyses of phosphonium salts with complex counterions ($X^- = BF_4^-$ or SbF_6^-), while photolyses of phosphonium halides $Ar_2CH\text{-}PPh_3^+X^-$ ($X^- = Cl^-$ or Br^-) in CH_2Cl_2 yield benzhydryl radicals $Ar_2CH^\bullet$ due to photo-electron transfer in the excited phosphonium halide ion pair. At low concentrations in CH_3CN, the precursor salts are mostly unpaired, and the photo-cleavage mechanism is independent of the nature of the counter-anions. Dichloromethane is better suited for generating the more reactive benzhydryl cations than the more polar and more nucleophilic solvents CH_3CN or CF_3CH_2OH. Efficient photo-generation of the most reactive benzhydryl cations $(3,5\text{-}F_2\text{–}C_6H_3)_2CH^+$ and $(4\text{-}(CF_3)\text{-}C_6H_4)_2CH^+$ was only achieved using the photo-leaving group $P(p\text{-Cl-}C_6H_4)_3$ and the counter-anion SbF_6^- in CH_2Cl_2. The lifetimes of the photogenerated benzhydryl cations depend greatly on the decay mechanisms, which can be reactions with the solvent, with the photo-leaving group PAr_3, or with the counter-anion X^- of the precursor salt. However, the nature of the photo-leaving group and the counterion of the precursor phosphonium salt do not affect the rates of the reactions of the obtained benzhydryl cations toward added nucleophiles. The method presented in this work allows us to generate a wide range of donor- and acceptor-substituted benzhydryl cations Ar_2CH^+ for the purpose of studying their electrophilic reactivities.

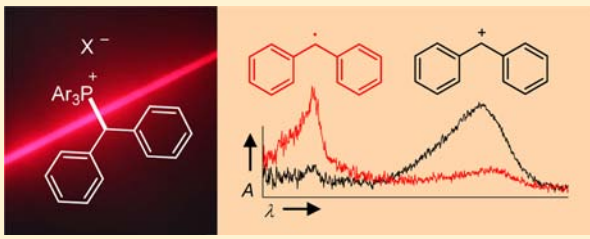

1. INTRODUCTION

The photolytic generation of carbocations by heterolytic cleavage of neutral (R-X) and charged ($R\text{-}X^+$) precursors has been employed not only for studying the rates of fast reactions of carbocations with nucleophiles[1−19] but also for the photo-initiation of carbocationic polymerizations.[20] Furthermore, photogenerated carbenium ions are the initial cleavage products of the photolysis of certain photoacid and photobase generators.[21−26] Common precursors for such applications are halides R-Hal,[2−5,21a,27] acetates R-OAc,[6−10,28] aryl ethers,[6−9] and onium salts such as halonium,[25,29] sulfonium,[21b,25,30] ammonium,[2,11,14,22,31] and phosphonium salts.[14−20,23,32−34] Heterolytic bond cleavages are often accompanied by formation of radicals via homolytic processes, particularly when the resulting carbocations are not highly stabilized and less polar solvents are employed.[35]

Among the many photo-leaving groups, phosphines turned out to be particularly advantageous, because they combine high stability,[36] even in alcoholic and aqueous solution, with a high preference for heterolytic cleavage and low tendency to produce radicals.[14−20,32−34,38] While we have recently reported several examples for the photolytic generation of carbocations from quaternary phosphonium salts,[14−19] there was no systematic investigation about the relationship between the structure of the precursor salt and the yields of the generated carbocations. The lack of information became obvious when we failed to generate benzhydrylium ions with empirical electrophilicity parameters $E > 7$ by laser flash photolysis of phosphonium salts $Ar_2CH\text{-}PPh_3^+BF_4^-$. As the photolytic generation of highly electrophilic carbocations is of general importance, we have now examined how the efficiency of carbocation formation can be influenced by the reactivity of the photo-electrofuge (carbocation-to-be), the photo-nucleofuge (photo-leaving group), and the counterion of

Received: February 22, 2012
Published: May 15, 2012

 © 2012 American Chemical Society

the phosphonium salt. To gain insight into the ultrafast dynamics of these processes, the nanosecond laser flash photolysis experiments are supplemented by experiments on a state-of-the-art femtosecond transient spectrometer.[39]

The use of benzhydryl derivatives is advantageous for these investigations because of the clearly assignable distinct spectra of the resulting cations and radicals.[40] Benzhydryl cations furthermore do not have β-protons and therefore cannot eliminate H^+, which reduces the number of subsequent processes.[15] Moreover, a systematic variation of the reactivity of the generated carbocations is achieved by using substituted benzhydryl cations Ar_2CH^+ ($\mathbf{E}^+$) whose electrophilic reactivities are quantified accurately by the empirical electrophilicity parameters E.[41]

In the following, we will first investigate how the yields and dynamics of the photoproducts change with variations of the benzhydryl (section 3.2) and phosphine moieties (section 3.3) of the precursor molecules, of the solvent (section 3.4), and of the counter-anions of the phosphonium salts (section 3.5). We will then show how this information can be employed to generate highly reactive carbocations such as $\mathbf{E(18-20)}^+$ (section 3.6). After discussing how the reaction conditions affect the lifetimes of the carbocations on the >10 ns time scale (section 3.7), we will finally demonstrate that the method presented in this work is well suitable for the study of bimolecular reactions of the generated benzhydryl cations (section 3.8).

2. EXPERIMENTAL SECTION

2.1. Materials. *Solvents.* For the nanosecond laser flash photolysis experiments, p.a. grade dichloromethane (Merck) was subsequently treated with concentrated sulfuric acid, water, 10% $NaHCO_3$ solution, and again water. After predrying with anhydrous $CaCl_2$, it was freshly distilled over CaH_2. Commercially available CH_2Cl_2 (Merck, spectrophotometric grade) was used for the ultrafast measurements because reactions with impurities are too slow to be observed on the picosecond time scale. Acetonitrile (HPLC grade, VWR or spectrophotometric grade, Sigma-Aldrich) and 2,2,2-trifluoroethanol (99%, Apollo) were used as received.

Phosphonium Salts. The phosphonium salts $\mathbf{E}$-$PAr_3^+X^-$ were prepared by heating Ar_2CH-OH with $Ph_3PH^+X^-$ or by treating Ar_2CH-Br with PAr_3 and subsequent anion metathesis.[42]

2.2. Laser Flash Photolysis. *Nanosecond Laser Flash Photolysis.* Solutions of $\mathbf{E}$-$PAr_3^+X^-$ ($A_{266\,nm} \approx 0.1-1.0$, ca. 5×10^{-5} to 10^{-4} M) were irradiated with a 7-ns laser pulse from the fourth harmonic of a Nd/YAG laser (λ_{exc} = 266 nm, 30−60 mJ/pulse, diameter ~1 cm). A xenon lamp was used as probe light for UV/vis detection (d = 1 cm). Transient spectra were obtained as difference spectra from subsequent determinations with and without laser pulse using an ICCD camera with 10 ns gate width; i.e., the ns time scale spectra published in this work show the average of the transient signals during the first 10 ns after the laser pulse. To reduce noise, 4−16 such spectra were averaged, whereby the solutions of the substrates were replaced completely between subsequent laser pulses by using a flow cuvette.

Decay kinetics of the benzhydryl cations $\mathbf{E}^+$ were measured by following the absorbances A at λ_{max}; typically ≥64 individual decay curves were averaged. The decay rate constants k_{obs} (s^{-1}) were obtained from the averaged curve by least-squares fitting to the single-exponential function $A(t) = A_0\,e^{-k_{obs}t} + C$. The non-exponential decays were evaluated with the software Gepasi.[43]

Femtosecond UV/Vis Transient Absorption Measurements. The employed broadband transient absorption spectrometer is described in detail in ref 39. Solutions of $\mathbf{E}$-$PAr_3^+X^-$ ($A_{280\,nm} \approx 0.1-0.3$, ca. 4×10^{-4} to 6×10^{-3} M) were pumped through a flow cell of 120 μm or 1 mm thickness and irradiated with 35-fs pulses (λ_{exc} = 280 nm, 200 nJ/pulse) from the frequency-doubled output of a noncollinear optical parametric amplifier (NOPA). The pulses were focused down to a diameter of about 100 μm inside the sample. A CaF_2 white light continuum spanning from 290 to 700 nm and polarized at the magic angle was used as probe light.

The time-dependent transient spectra were recorded with temporal resolutions between 100 and 400 fs, depending on the thickness of the sample layer, but always well below all observed decay rates. The decay kinetics were followed at λ_{max} of the benzhydryl cations or radicals. The absorbances were converted to quantum yields using the absorption coefficients of the benzhydryl cations[40] and the accurately determined excitation probability.[39] A least-squares fit of the time-dependent absorbances $A(t)$ to the sum of exponential curves and a constant provided the decay rate constants and amplitudes from which the quantum yields and rate constants for the different processes were derived (see Supporting Information for details).

3. RESULTS AND DISCUSSION

3.1. General. Scheme 1 shows a mechanism for the photogeneration of benzhydryl cations $\mathbf{E}^+$ and benzhydryl radicals $\mathbf{E}^\bullet$

Scheme 1. Generation of Benzhydryl Cations $\mathbf{E}^+$ and Benzhydryl Radicals $\mathbf{E}^\bullet$ by Photolysis of Phosphonium Ions $\mathbf{E}$-PPh_3^+

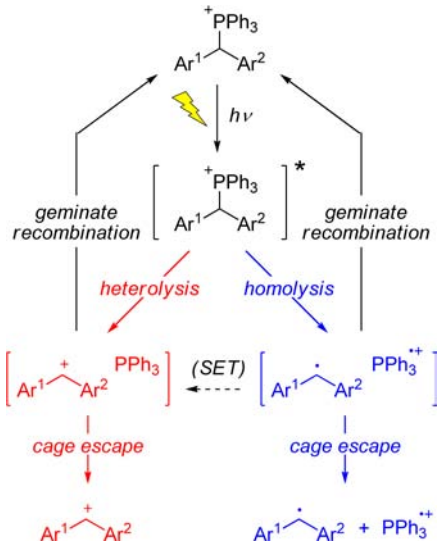

from benzhydryl phosphonium ions $\mathbf{E}$-PPh_3^+ in line with previously proposed mechanisms for similar systems.[35] The excited precursor molecules can either undergo heterolytic bond cleavage to the carbocation/triphenylphosphine pair [$\mathbf{E}^+$ PPh_3] (red pathway) or homolytic bond cleavage to the radical pair [$\mathbf{E}^\bullet PPh_3^{\bullet+}$] (blue pathway). Both pairs can then either undergo geminate recombination to the starting material or diffusional separation, which results in the free benzhydryl cations $\mathbf{E}^+$ or radicals $\mathbf{E}^\bullet$. Only the UV/vis-absorbing species which escape the geminate solvent cage ($\mathbf{E}^+$, $\mathbf{E}^\bullet$, and $PR_3^{\bullet+}$; bottom line of Scheme 1) have sufficient lifetimes (>10 ns) to be observed spectroscopically with a nanosecond laser flash setup.

3.2. Effect of the Photo-electrofuge (i.e., Structure of the Benzhydrylium Ion). *Nanosecond Spectroscopy in CH_2Cl_2.* The transient spectra which we obtained by irradiation of 10^{-5}−10^{-4} M solutions of $\mathbf{E(1-20)}$-$PPh_3^+BF_4^-$ in CH_2Cl_2 with a 7-ns laser pulse (266 nm, 30−60 mJ/pulse) are compiled in section S3 of the Supporting Information; four characteristic examples are shown in Figure 1. The transient spectra feature three types of absorption bands: (i) broad bands with λ_{max} = 426−535 nm, which can be assigned to the cations $\mathbf{E}^+$ by comparison with the previously reported spectra of benzhydrylium ions,[40] and the cation-like reactivities (see below); (ii)

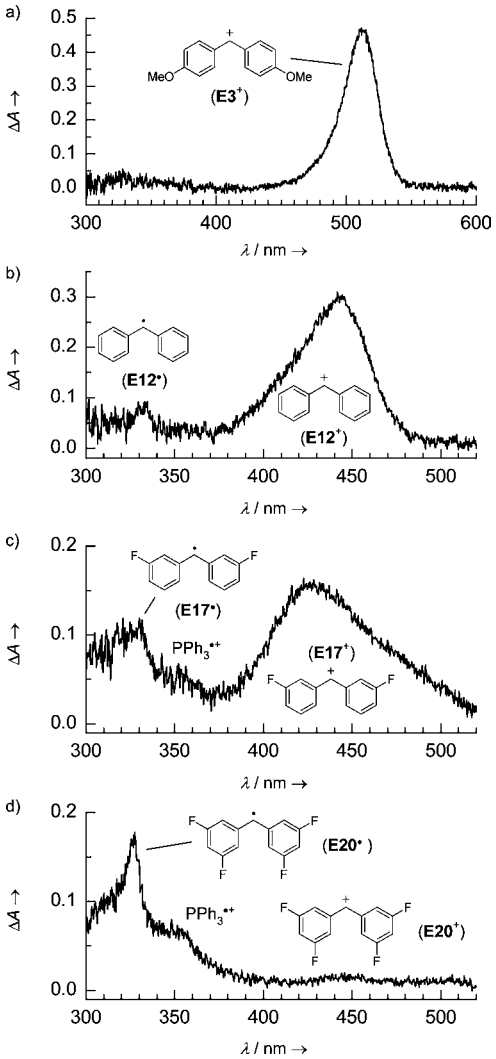

Figure 1. Transient spectra obtained after irradiation (7-ns pulse, λ_{exc} = 266 nm, gate width = 10 ns) of CH_2Cl_2 solutions of benzhydryl triphenylphosphonium tetrafluoroborates: (a) **E3**-$PPh_3^+BF_4^-$ ($A_{266\,nm}$ = 0.16), (b) **E12**-$PPh_3^+BF_4^-$ ($A_{266\,nm}$ = 0.49), (c) **E17**-$PPh_3^+BF_4^-$ ($A_{266\,nm}$ = 0.90), (d) **E20**-$PPh_3^+BF_4^-$ ($A_{266\,nm}$ = 0.64).

sharp bands with λ_{max} = 328−344 nm, which closely resemble the published spectra of benzhydryl radicals $\mathbf{E}^\bullet$ in CH_3CN;[40] and (iii) a shoulder at ca. 350−360 nm, which we assign to the triphenylphosphine radical cation $PPh_3^{\bullet+}$, in agreement with its reported spectrum in CH_2Cl_2 solution (with $\lambda_{max} \approx$ 330 nm).[44]

The photo-cleavage of the phosphonium ions **E(1−9)**-PPh_3^+ in CH_2Cl_2 yields the stabilized benzhydrylium ions **E(1−9)**$^+$ exclusively. When we irradiated solutions of **E(10−20)**-$PPh_3^+BF_4^-$ in CH_2Cl_2, the ratios of the absorbances of the benzhydryl cations $\mathbf{E}^+$ and benzhydryl radicals $\mathbf{E}^\bullet$ decreased with increasing electrophilicity E of the carbocations (Table 1). The least stable carbocations in the series, **E(18−20)**$^+$ are hardly detectable after photolysis of **E(18−20)**-$PPh_3^+BF_4^-$, and the radicals **E(18−20)**$^\bullet$ are obtained almost exclusively (Figure 1d and Figure S3 in the Supporting Information).

Picosecond Dynamics in CH_2Cl_2. The processes which lead to the formation of $\mathbf{E}^+$ and $\mathbf{E}^\bullet$ are too fast to be followed with the nanosecond laser flash photolysis instrument. A closer look at these processes is provided by transient absorption measurements with sub-100-fs time resolution which we performed for selected benzhydryl triarylphosphonium salts. Figure 2 shows a

Table 1. Electrophilicity Parameters E of the Benzhydryl Cations E(1-20)$^+$ and Absorption Maxima λ_{max} (nm) of Benzhydryl Radicals $\mathbf{E}^\bullet$ and Benzhydryl Cations $\mathbf{E}^+$ in CH_2Cl_2

no.	X	Y	E ($\mathbf{E}^+$)[a]	λ_{max} / nm $\mathbf{E}^\bullet$	λ_{max} / nm $\mathbf{E}^+$	absorbance ratio[b]
E1$^+$	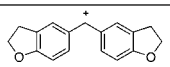		−1.36	[c]	535	[c]
E2$^+$	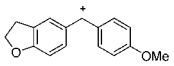		−0.81[d]	[c]	524	[c]
E3$^+$	4-MeO	4-MeO	0.00	[c]	513	[c]
E4$^+$	4-MeO	4-PhO	0.61	[c]	517	[c]
E5$^+$	4-MeO	4-Me	1.48	[c]	484	[c]
E6$^+$	4-MeO	H	2.11	[c]	466	[c]
E7$^+$	4-PhO	H	2.90	[c]	473	[c]
E8$^+$	4-Me	4-Me	3.63	[c]	473	[c]
E9$^+$	4-Me	H	4.43[d]	[c]	456	[c]
E10$^+$	4-F	4-F	5.01[d]	~327	447	≥ 7
E11$^+$	4-F	H	5.20[d]	~333	451	≥ 5
E12$^+$	H	H	5.47[d]	~332	443	~4
E13$^+$	4-Cl	4-Cl	5.48[d]	~344	480	~4
E14$^+$	3-F	H	6.23[d]	~337	438	~3
E15$^+$	4-(CF_3)	H	6.70[d]	~338	430	~2
E16$^+$	3,5-F_2	H	6.74[d]	~332	434	~1.7
E17$^+$	3-F	3-F	6.87[d]	~331	426	~1.5
E18$^+$	3,5-F_2	3-F	7.52[d]	~328	435	~0.25
E19$^+$	4-(CF_3)	4-(CF_3)	(7.96)[d,e]	~337	439	<0.1
E20$^+$	3,5-F_2	3,5-F_2	(8.02)[d,e]	~328	445	<0.1

[a]Electrophilicity parameters E of the benzhydryl cations $\mathbf{E}^+$; from ref 41a unless noted otherwise. [b]Ratio of absorbances at λ_{max} ($\mathbf{E}^+$) and at λ_{max} ($\mathbf{E}^\bullet$) obtained by laser flash photolysis (7-ns pulse, λ_{exc} = 266 nm) of **E(1−20)**-$PPh_3^+BF_4^-$ in CH_2Cl_2. Due to the overlap with the $PPh_3^{\bullet+}$ band, absorbances at λ_{max} ($\mathbf{E}^\bullet$) overestimate the amount of radicals present. [c]No radicals detected. [d]New or revised E parameters from unpublished work. [e]Approximate values.

false color representation of the ps transient absorption data obtained by irradiating **E12**-$PPh_3^+BF_4^-$ in CH_2Cl_2 with a ~35-fs pulse (280 nm, 200 nJ/pulse): The wavelength is plotted on the horizontal axis and the time after the laser pulse on the vertical axis. Blue color indicates low absorbance and red color high absorbance.

The plot features three types of bands: (i) a broad absorption band below 400 nm, which disappears in the first 30 ps, is assigned to the excited state absorption (ESA) of the phosphonium salt precursor; (ii) the band of the benzhydryl cation **E12**$^+$ ($\lambda_{max} \approx$ 443 nm), which reaches a maximum within the first 25 ps; and (iii) a small band of the benzhydryl radical **E12**$^\bullet$ ($\lambda_{max} \approx$ 332 nm), which becomes visible after the decay of the excited state of the phosphonium ion. The graph to the right of the color plot shows the dynamics of the absorbance at λ_{max} of the carbocation **E12**$^+$ (red) and at 332 nm (blue), λ_{max} of the radical **E12**$^\bullet$ overlapping with the excited-state absorption in the first tens of picoseconds.

The intense short-lived (<0.1 ps) signal directly after the laser pulse is a coherent artifact that is also observed in the pure

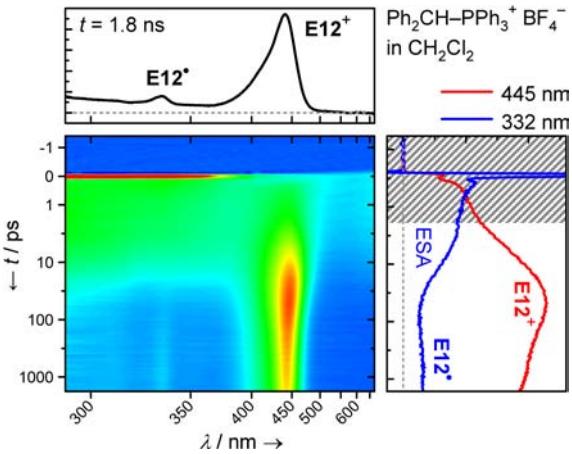

Figure 2. Transient absorptions observed after irradiating a 5.2×10^{-3} M solution of **E12**-$PPh_3^+BF_4^-$ in CH_2Cl_2 by a 35-fs pulse (λ_{exc} = 280 nm, $A_{280\ nm}$ = 0.2, d = 120 μm). The graph above the color plot shows the spectrum after 1.8 ns (black). The graph on the right shows the dynamics of the absorbances at selected wavelengths: Absorbance of benzhydryl cation **E12**$^+$ (445 nm, red); and absorbance of the excited state (ESA) of the phosphonium ion and the benzhydryl radical **E12**$^\bullet$ (332 nm, blue). The time scale is linear between −1 and +1 ps and logarithmic above 1 ps.

solvent and will be ignored in the following.[39] A discussion of the absorption changes during the first 2 ps (shaded area) which include relaxation, planarization, and solvation effects is beyond the scope of this paper and is treated in detail elsewhere.[45]

The ESA disappears during the first 30 ps, accompanied by a simultaneous increase of the absorbance of **E12**$^+$ which suggests that **E12**$^+$ is formed by direct heterolysis of the excited precursor salt. It does not, however, exclude the generation of the benzhydryl cations **E12**$^+$ by homolytic bond cleavage and subsequent considerably faster single electron transfer (SET) in the geminate radical pair (Scheme 1, dashed arrow).

After the ESA has disappeared and the absorbance of **E12**$^+$ has reached its maximum, the population of **E12**$^+$ decreases as a result of the geminate recombination of **E12**$^+$ with the photo-leaving group PPh_3; in part, the photo-fragments diffuse away from each other and these **E12**$^+$ persist on this time scale. Once the band of the radical **E12**$^\bullet$ is clearly developed, it does not show noticeable dynamics. After 1.8 ns, we observe the spectrum shown in the graph above the color plot (Figure 2), which is essentially the same as the spectrum obtained by the 7-ns laser pulse (Figure 1b).

The corresponding plot for the photolysis of the tetrafluoro-substituted benzhydryl phosphonium ion **E20**-$PPh_3^+BF_4^-$ in CH_2Cl_2 is shown in Figure S4.1 in the Supporting Information. The heterolysis of this precursor is much less effective and the radical **E20**$^\bullet$ is formed predominantly. In addition, the small initial concentration of carbocations **E20**$^+$ decays rapidly so that only a very low concentration can be observed on the nanosecond time scale (Figure 1d; also see Table 2).[46]

Picosecond Dynamics in CH_3CN. Figure S4.2 in the Supporting Information illustrates that in CH_3CN essentially the same kind of photo-processes occur after irradiation of **E12**-$PPh_3^+BF_4^-$ as in CH_2Cl_2 (Figure 2). Figure 3 shows the time-dependent quantum yields of the substituted benzhydryl cations **E**$^+$ during the first 1.6 ns after the excitation pulse; the numeric values are listed in Table 2. It is evident that the quantum yields of the initial heterolytic photo-cleavage, Φ_{het}, decrease with increasing electrophilicity of the generated benzhydryl cations. At the same time, homolytic bond cleavage becomes more favorable although the overall efficiency of bond cleavage decreases (not shown). Due to the overlap of the bands of **E**$^\bullet$ with the ESA and the $PAr_3^{\bullet+}$ band we could not evaluate the radical yields on the early picosecond time scale.

As illustrated by Figure 3, the concentrations of the benzhydryl cations **E**$^+$ decrease considerably during the first 300 ps after their formation which is rationalized by the geminate recombination with the photo-leaving group PPh_3. Immediately after C−P bond cleavage, the two photofragments are in close vicinity (ion pairs).

Table 2. Yields and Rate Constants Associated with the Dynamics of E$^+$ after Irradiation of E-$PAr_3^+BF_4^-$ with Ar = Ph or *p*-Cl-C_6H_4 (Bold) in CH_3CN or CH_2Cl_2 with a 35-fs Laser Pulse (λ_{exc} = 280 nm)[a]

E$^+$	E(E$^+$)[b]	PAr_3	solvent	Φ_{het}[c] (%)	Y_{recomb}[d] (%)	Φ_{free}[e] (%)	k_{recomb}[f] (s^{-1})	k_{esc}[g] (s^{-1})
E8$^+$	3.63	PPh_3	CH_3CN	34	21	27	1.9×10^9	7.2×10^9
E9$^+$	4.43	PPh_3	CH_3CN	30	25	23	2.5×10^9	7.5×10^9
E12$^+$	5.47	PPh_3	CH_3CN	24	25	18	2.7×10^9	8.3×10^9
			CH_2Cl_2	*11*	*19*	*9*	*1.1×10^9*	*4.9×10^9*
		P(*p*-Cl-C_6H_4)$_3$	**CH_3CN**	**25**	**21**	**20**	**7.9×10^8**	3.0×10^9
			CH_2Cl_2	***(~16)***[h]	***(~10)***[h]	***14***	***(6×10^8)***[h]	***(5×10^9)***[h]
E14$^+$	6.23	PPh_3	CH_3CN	6−10[i]	29	4−7[i]	3.6×10^9	8.5×10^9
E17$^+$	6.87	PPh_3	CH_3CN	5−8[i]	32	3−5[i]	3.6×10^9	7.5×10^9
E18$^+$	7.52	PPh_3	CH_3CN	4−7[i]	35	3−4[i]	3.8×10^9	6.9×10^9
		P(*p*-Cl-C_6H_4)$_3$	**CH_3CN**	**8−12[i]**	**36**	**5−7[i]**	**8.9×10^9**	**1.6×10^{10}**
E20$^+$	(8.02)	PPh_3	CH_3CN	3−4[i]	42	~2[i]	6.6×10^9	9.3×10^9
			CH_2Cl_2	*(~1)*[i,j]	*(29)*[j]	*(≤1)*[i,j]	*(2×10^9)*[j]	*(5×10^9)*[j]
		P(*p*-Cl-C_6H_4)$_3$	**CH_3CN**	**8−12[i]**	**36**	**5−8[i]**	**8.8×10^9**	**1.6×10^{10}**

[a]See section S5 in the Supporting Information for details. [b]Electrophilicity parameters E of the benzhydryl cations **E**$^+$; see Table 1 for references. [c]Quantum yield of heterolytic bond cleavage (including the possibility of initial homolytic bond cleavage and subsequent fast electron transfer). [d]Yield of geminate recombination of **E**$^+$ with the phosphine PAr_3. [e]Overall quantum yield of free **E**$^+$ (at ~2 ns) after diffusional separation of the photo-leaving group. [f]First-order rate constant for the geminate recombination of **E**$^+$ with PAr_3. [g]First-order rate constant for the diffusional separation of **E**$^+$ and PAr_3. [h]The different behavior of this photo-leaving group in the early photo-dissociation process in CH_2Cl_2 reduces the accuracy of our fit and we give only approximate values for this system. [i]To calculate the quantum yields, absorbance coefficients of $(5.0-7.5) \times 10^4$ M^{-1} cm^{-1} were assumed for the benzhydryl cations **E(14,17,18,20)**$^+$ in analogy to reported values for similar benzhydrylium ions.[40] [j]The values have to be considered approximate because of the low absorbance of **E20**$^+$.

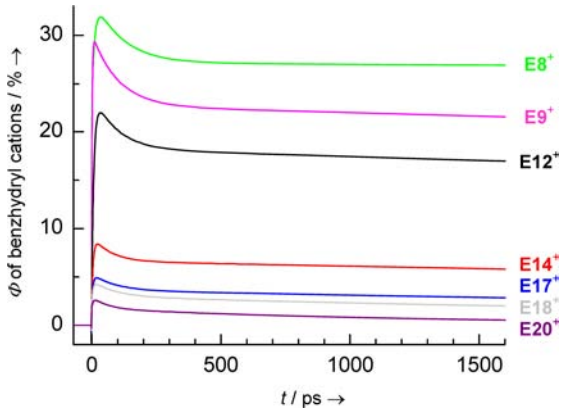

Figure 3. Time-dependent quantum yields Φ of E^+ observed after irradiation of **E**-$PPh_3^+BF_4^-$ solutions in CH_3CN with a 35-fs laser pulse (λ_{exc} = 280 nm).

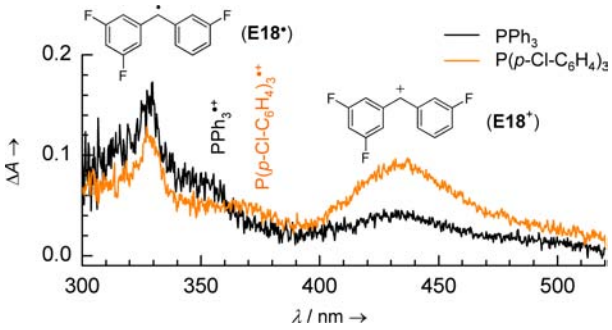

Figure 4. Transient spectra obtained after irradiation (7-ns pulse, λ_{exc} = 266 nm, gate width: 10 ns) of CH_2Cl_2 solutions of benzhydryl triarylphosphonium tetrafluoroborates **E18**-$PAr_3^+BF_4^-$ with different photoleaving groups PAr_3 = PPh_3 (black, $A_{266\,nm}$ = 1.0) and PAr_3 = P(*p*-Cl-C_6H_4)$_3$ (orange, $A_{266\,nm}$ = 1.0).

They can either undergo geminate recombination or the fragments diffuse apart. After complete diffusional separation of E^+ from the photo-leaving group, bond formation is no longer possible (more precisely: is too slow to be observable on this time scale) and the absorbances of E^+ reach a plateau (Figure 3). The yields for the geminate recombination of the benzhydryl cations E^+ with the phosphine PPh_3, Y_{recomb}, increase with the electrophilicity *E* of the carbocations E^+, and diminish the final quantum yields of the diffusionally separated (free) benzhydryl cations, Φ_{free} (Table 2).

The rate constants listed in Table 2 for the geminate recombination of E^+ with PPh_3, k_{recomb} (s^{-1}), and for the diffusional separation of E^+ from PPh_3, k_{esc} (s^{-1}), can be derived from $Y_{recomb} = k_{recomb}/(k_{recomb}+k_{esc})$ and the observed rate constants for the decrease of the benzhydrylium ions (see section S5 in the Supporting Information for details). With increasing electrophilicity *E* of the benzhydryl cations E^+, the recombination rate constant k_{recomb} increases steadily while k_{esc} remains almost constant at $(7-9) \times 10^9\ s^{-1}$.

3.3. Effect of the Photo-nucleofuge (i.e., Triarylphosphine). It was already observed by Modro and co-workers that the use of a more nucleophilic phosphine as photo-leaving group decreased the amount of cation-derived photo-products in photolyses of phosphonium salts.[32] When we employed tris(4-chlorophenyl)phosphine P(*p*-Cl-C_6H_4)$_3$ as a photo-leaving group instead of PPh_3, the formation of benzhydryl cations E^+ was considerably more efficient and even allowed us to generate highly electrophilic benzhydrylium ions.

Figure 4 shows the transient spectra obtained after irradiation of the benzhydryl triarylphosphonium tetrafluoroborates **E18**-$PAr_3^+BF_4^-$ with PAr_3 = PPh_3 (black curves) and PAr_3 = P(*p*-Cl-C_6H_4)$_3$ (orange curves). Considerably higher concentrations of the carbocations $E18^+$ and lower amounts of the radicals $E18^\bullet$ were obtained when P(*p*-Cl-C_6H_4)$_3$ was employed as photo-leaving group. Similarly, irradiation of **E20**-P(*p*-Cl-C_6H_4)$_3^+BF_4^-$ gave higher yields of $E20^+$ and lower yields of $E20^\bullet$ than irradiation of **E20**-$PPh_3^+BF_4^-$, but the absorbance of $E20^+$ was still too low (A < 0.04) to study its reaction rates on the nanosecond time scale. The shoulders of the radical bands ($PAr_3^{\bullet+}$) are weaker and red-shifted to 350−380 nm when P(*p*-Cl-C_6H_4)$_3$ is used as photo-leaving group (Figure 4), in agreement with the fact that the absorbance maxima of the tris(4-chlorophenyl)phosphine radical cation P(*p*-Cl-C_6H_4)$_3^{\bullet+}$ are slightly red-shifted compared to $PPh_3^{\bullet+}$.[47]

Two reasons might account for the increased carbocation yields with P(*p*-Cl-C_6H_4)$_3$ as photo-leaving group: First, the oxidation potentials of the two phosphines (E^0_{ox} = 1.06 V for PPh_3 and 1.28 V for P(*p*-Cl-C_6H_4)$_3$ in CH_3CN)[48] indicate a higher thermodynamic preference of E^+/PAr_3 pairs over $E^\bullet/PAr_3^{\bullet+}$ pairs in the case of P(*p*-Cl-C_6H_4)$_3$ than in the case of PPh_3. Thus, the preference for the heterolytic over the homolytic pathway should be larger for **E**-P(*p*-Cl-C_6H_4)$_3^+$ than for **E**-PPh_3^+. Furthermore, P(*p*-Cl-C_6H_4)$_3$ is less nucleophilic than PPh_3 (ΔN = 1.75)[37] and, therefore, allows more carbocations to undergo diffusional separation instead of geminate recombination.

The data from the ultrafast spectroscopic measurements illustrate that both effects contribute to the better overall quantum yields Φ_{free} when P(*p*-Cl-C_6H_4)$_3$ is used as photo-leaving group instead of PPh_3 (Table 2, bold entries): For this leaving group, the observed initial quantum yields of the heterolytic bond cleavage, Φ_{het}, are higher and the yields of the geminate recombination, Y_{recomb}, are lower. While the differences are small for the photolysis of **E12**-$PAr_3^+BF_4^-$ in CH_3CN, the effects are more important in CH_2Cl_2 and crucial for the generation of the most reactive benzhydryl cations (Table 2).

3.4. Effect of Solvent on the Picosecond Dynamics. The overall quantum yields of the free carbocations, Φ_{free}, are considerably lower in CH_2Cl_2 than in CH_3CN (Table 2), which is a consequence of the decreased quantum yields for the heterolytic bond cleavage, Φ_{het}. The lower solvent nucleophilicity of CH_2Cl_2 compared to CH_3CN only becomes relevant at longer time scales (see below).

The rate constants for the cage escape, k_{esc}, are of comparable magnitude in CH_2Cl_2 and CH_3CN for both photo-nucleofuges PAr_3 (Table 2). In contrast, the diffusional separation of E^+ from Cl^- is very slow after the photolysis of **E**-Cl in CH_2Cl_2 due to the Coulombic attraction between the charged photo-fragments,[4] which explains why photolyses of **E**-PAr_3^+ give much higher yields of carbocations in CH_2Cl_2 than photolyses of **E**-Cl.

3.5. Effect of the Counterion in the Precursor Phosphonium Salt. *Transient Spectra in CH_3CN and CH_2Cl_2.* At low phosphonium salt concentrations (~1 × 10^{-4} M), the association equilibria of **E12**-$PPh_3^+X^-$ in acetonitrile are entirely on the side of the free (unpaired) ions.[42] Since the lifetime of the excited state is only a few ps, which is too short for the diffusive approach of external X^-, the photochemistry of **E12**-PPh_3^+ is not affected by the counter-anion X^- under these conditions.

Accordingly, ~1.2 × 10^{-4} M solutions of **E12**-$PPh_3^+X^-$ with different counter-anions X^- in CH_3CN gave very similar transient spectra upon irradiation with a 7-ns laser pulse (Figure 5a): Irrespective of the counter-anion X^-, the predominant photoproduct was the benzhydrylium ion **E12**$^+$ (λ_{max} ≈ 436 nm) together with small amounts of the radical **E12**$^\bullet$ (λ_{max} ≈ 329 nm). Since the absorption coefficients of **E12**$^+$ and **E12**$^\bullet$ are similar,[40] the absorbance ratios in Figure 5 directly translate to concentration ratios. The slightly lower concentrations of **E12**$^+$ obtained from precursors with X^- = Cl^- or Br^- (Figure 5a) result from the diffusion-controlled trapping of **E12**$^+$ by the halide ions (see below),[7] which can already be noticed on this time scale (first 10 ns).

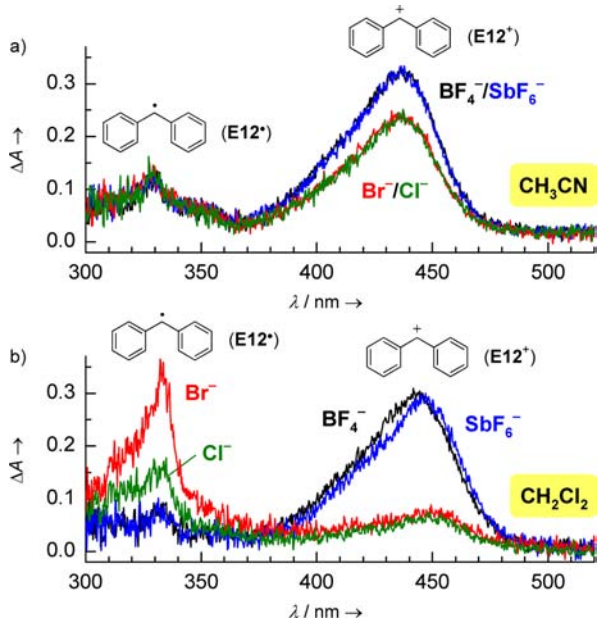

Figure 5. Transient spectra obtained by irradiation of **E12**-$PPh_3^+X^-$ ($A_{266\ nm}$ = 0.5, (1.0−1.2) × 10^{-4} M) with different counterions X^- = BF_4^- (black), SbF_6^- (blue), Br^- (red) or Cl^- (green) in CH_3CN (a) and CH_2Cl_2 (b) with a 7-ns laser pulse (λ_{exc} = 266 nm, gate width: 10 ns).

In CH_2Cl_2, the phosphonium salts **E12**-$PPh_3^+X^-$ have a considerably higher tendency to form ion pairs. At concentrations of 1 × 10^{-4} M, which we typically used in the nanosecond laser flash photolysis experiments, ~57% of the Cl^-, ~43% of the Br^-, ~40% of the BF_4^-, and roughly (10−30)% of the SbF_6^- salts exist as ion pairs in CD_2Cl_2.[42] When we irradiated solutions of **E12**-$PPh_3^+BF_4^-$ in CH_2Cl_2, we obtained mostly the benzhydrylium ion **E12**$^+$ (λ_{max} ≈ 443 nm) together with small amounts of the radical **E12**$^\bullet$ (λ_{max} ≈ 332 nm) (Figure 5b, black curve). Irradiation of CH_2Cl_2 solutions of **E12**-$PPh_3^+SbF_6^-$ gave almost the same concentrations of **E12**$^+$ and **E12**$^\bullet$ as the tetrafluoroborate precursor (Figure 5b, blue curve). In contrast, the concentration ratio of **E12**$^+$ and **E12**$^\bullet$ was reversed when we used the phosphonium bromide **E12**-PPh_3^+ Br^- as precursor (Figure 5b, red curve). Irradiation of the phosphonium chloride **E12**-PPh_3^+ Cl^- gave an intermediate amount of **E12**$^\bullet$ while the concentration of **E12**$^+$ was almost the same as with the phosphonium bromide precursor (Figure 5b, green curve). Transient spectra obtained by analogous experiments with **E12**-PPh_3^+ BPh_4^- are difficult to interpret because of the overlap with the absorbances of photoproducts derived from BPh_4^- and are discussed in section S6 in the Supporting Information.

Mechanism. The reduced yield of carbocations **E12**$^+$ obtained from the phosphonium halides in CH_2Cl_2 (Figure 5b) can in part be explained by the immediate combination of **E12**$^+$ with Br^- or Cl^- which are in close vicinity if they have been generated from the paired phosphonium halides. However, the increased yields of the radicals obtained from the phosphonium halides cannot be explained by the mechanism in Scheme 1 and subsequent reactions with the counterions, because Cl^- and Br^- do not reduce the benzhydrylium ions in the dark. Scheme 1, therefore, has to be extended as depicted in Scheme 2.

Scheme 2. Generation of Benzhydryl Cations E$^+$ and Benzhydryl Radicals E$^\bullet$ by Photolysis of Phosphonium Salts E-$PR_3^+X^-$ (R = Ph or *p*-Cl-C_6H_4): (a) Reactions of Unpaired Phosphonium Ions (Predominant Mechanism in CH_3CN) and (b) Reactions of Paired Phosphonium Ions (Predominant Mechanism in CH_2Cl_2)[a]

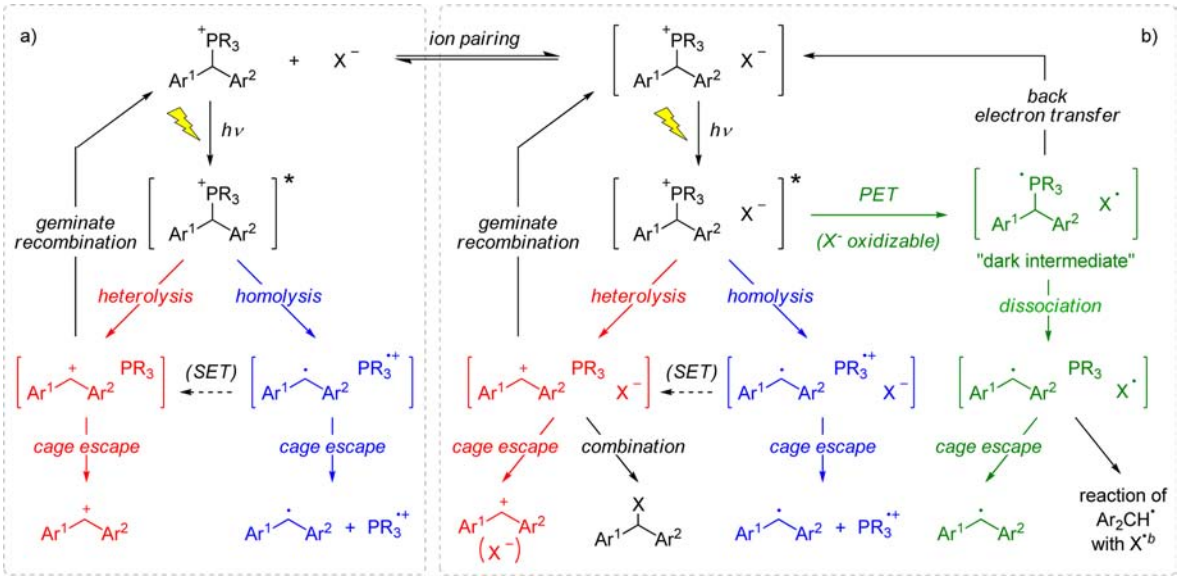

[a]For the sake of simplicity, the geminate recombination reactions for the radical pairs are not shown. [b]Radical combination or electron transfer.[4]

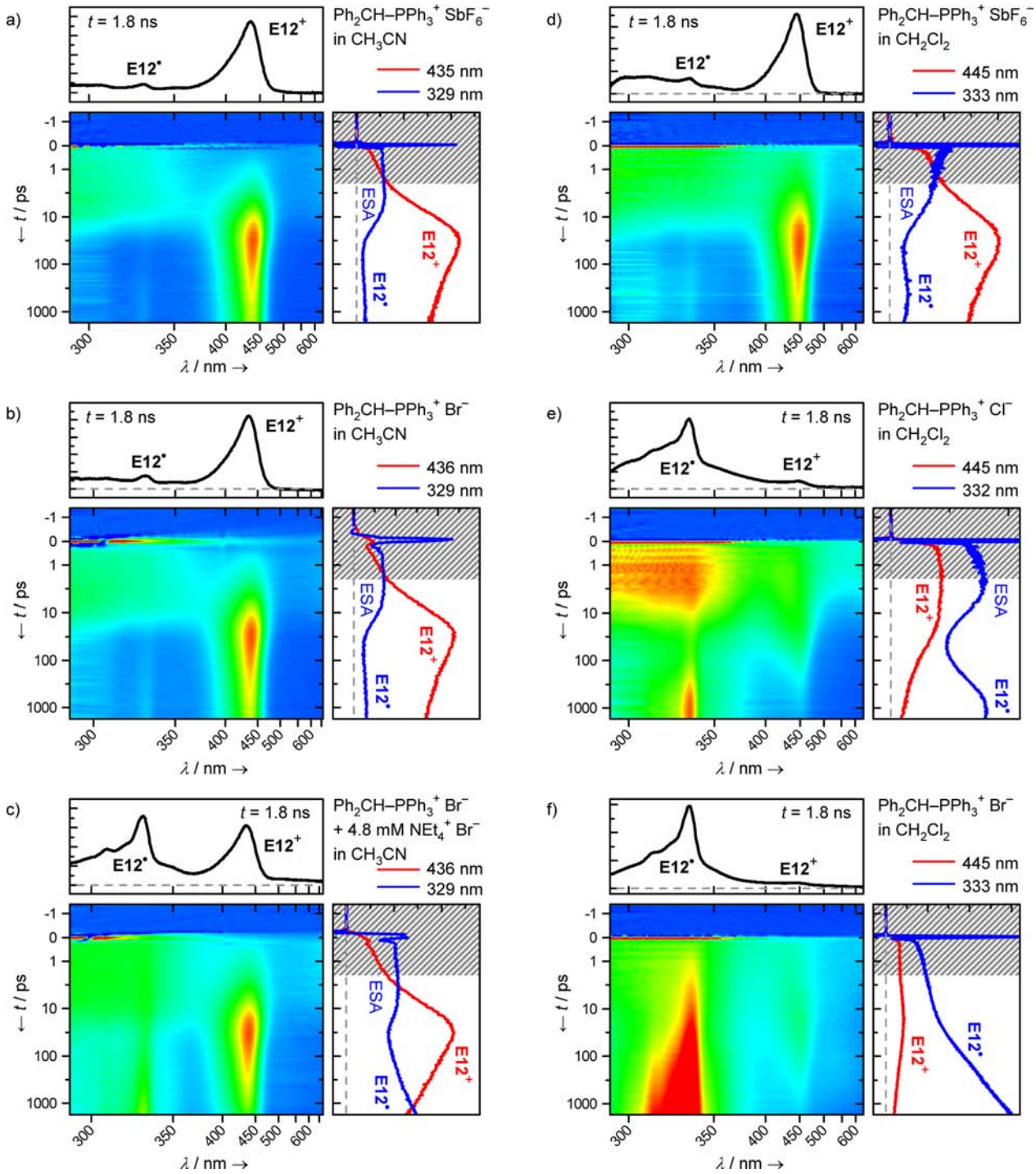

Figure 6. Transient absorptions obtained after irradiating solutions of **E12**-$PPh_3^+X^-$ with different counterions X^- in CH_3CN (a–c) and CH_2Cl_2 (d–f) by a 35-fs laser pulse (λ_{exc} = 280 nm). The graphs above the color plots show the spectra after 1.8 ns (black). The graphs on the right show the dynamics of the absorbances at certain wavelengths: absorbance of benzhydryl cation $\mathbf{E12}^+$ (436 or 445 nm, red) and absorbance of the excited state (ESA) and the benzhydryl radical $\mathbf{E12}^\bullet$ (329 or 333 nm, blue). (a) $X^- = SbF_6^-$ in CH_3CN; (b) $X^- = Br^-$ in CH_3CN; (c) $X^- = Br^-$ in CH_3CN with 4.8×10^{-3} M added $NEt_4^+Br^-$; (d) $X^- = SbF_6^-$ in CH_2Cl_2; (e) $X^- = Cl^-$ in CH_2Cl_2; (f) $X^- = Br^-$ in CH_2Cl_2. The color scales in the false color plots are comparable in Figures (a-f), but the absorbances in the small graphs (spectra and dynamics) were scaled to the available space and cannot be compared directly. The time scale is linear between −1 and +1 ps and logarithmic above 1 ps. For the reasons discussed in context of Figure 2, the absorption changes during the first 2 ps (shaded area) are discussed elsewhere.[45] Experimental conditions: (a,d–f) (5–7) × 10^{-3} M precursor ($A_{280\,nm}$ = 0.2), d = 120 μm; (b,c) 4 × 10^{-4} M precursor ($A_{280\,nm}$ = 0.1), d = 1 mm.

The phosphonium precursors can exist as free phosphonium ions or paired with the counter-anions. Like the unpaired phosphonium ions (Scheme 2a), the ion pairs can undergo heterolytic bond cleavage to the benzhydryl cations $\mathbf{E}^+$ (Scheme 2b, red pathway) or homolytic bond cleavage to the benzhydryl radicals $\mathbf{E}^\bullet$ (Scheme 2b, blue pathway). If the counter-anion is oxidizable, there is the additional possibility of a photo-electron transfer (PET) in the excited phosphonium ion pair (Scheme 2b,

green pathway). Such a PET was already proposed by Griffin et al.[49] and further substantiated by Modro and co-workers who suggested a mechanism similar to Scheme 2 for the photolysis of arylmethyl phosphonium salts with oxidizable counterions.[32,50] As expected for an electron transfer mechanism, the yields of the radicals **E12**$^{\bullet}$ obtained from **E12**-$PPh_3^+X^-$ increase with decreasing oxidation potentials of the counterions X^- ($Br^- < Cl^- \ll BF_4^-$ and SbF_6^-). Related to the degree of ion pairing of the precursor salts in these solvents,[42] Scheme 2a is the predominant pathway in CH_3CN and Scheme 2b predominates in CH_2Cl_2.

Our results agree with those of Johnston, Scaiano, and co-workers, who studied the photolyses of arylmethyl triphenylphosphonium *chlorides* in CH_3CN and other solvents under conditions where ion-pairing is not negligible.[33] They had already noticed that the concentrations of transient arylmethyl cations increased and the concentrations of radicals decreased when inorganic salts of non-nucleophilic anions (e.g., $LiClO_4$, $NaBF_4$) were added to the phosphonium chloride solutions, because these anions replace the Cl^- in the initial phosphonium salt ion pairs. As expected, this effect is larger in less polar solvents.[33]

Picosecond Dynamics in CH_3CN and CH_2Cl_2. The data from the ultrafast measurements corroborate this interpretation. Figure 6 shows the false color representations of the ps transient absorptions obtained after irradiation of **E12**-$PPh_3^+X^-$ with different counter-anions ($X^- = SbF_6^-$, Cl^-, and Br^-) in CH_3CN or CH_2Cl_2. The plots for **E12**-$PPh_3^+SbF_6^-$ in CH_3CN (Figure 6a) and CH_2Cl_2 (Figure 6d) are very similar to that of the tetrafluoroborate precursor (Figure 2) and can be interpreted analogously (see above). Likewise, the color plot obtained with 4×10^{-4} M **E12**-PPh_3^+ Br^- in CH_3CN (Figure 6b) closely resembles that of **E12**-$PPh_3^+SbF_6^-$ (Figure 6a), because ion pairing is negligible at these concentrations[42] and the PET mechanism depicted in Scheme 2b (green pathway) cannot occur. In all these cases, **E12**$^+$ is the predominant photo-product, and only very small amounts of **E12**$^{\bullet}$ are obtained.

At larger precursor concentrations or in the presence of added bromide, however, the association equilibrium of the precursor phosphonium salt is shifted toward the ion pairs, and the PET pathway becomes available also in CH_3CN. Figure 6c shows the false color plot obtained after irradiation of **E12**-PPh_3^+ Br^- in the presence of 4.8×10^{-3} M added NEt_4^+ Br^-. We now observed a significant amount of benzhydryl radicals **E12**$^{\bullet}$ while the yield of the benzhydryl cations **E12**$^+$ decreased.

The false color representations of the transient absorption data recorded after irradiation of **E12**-$PPh_3^+X^-$ with different counter-anions ($X^- = SbF_6^-$, Cl^-, and Br^-) in CH_2Cl_2 are shown in Figure 6d–f. As already discussed, the plot for **E12**-$PPh_3^+SbF_6^-$ (Figure 6d) is similar to that observed in CH_3CN. Irradiation of **E12**-$PPh_3^+Cl^-$ gave the color plot shown in Figure 6e, which is an intermediate case between the SbF_6^- and the Br^- salts. At any time, only a small amount of carbocations **E12**$^+$ is present. In addition, most of the initially generated **E12**$^+$ decay during the first 1.8 ns due to the combination reaction of **E12**$^+$ with Cl^-. The decay of the ESA is not associated with an increase of the carbocation absorbance, indicating that the excited state disappears predominantly by the PET mechanism and not by heterolytic bond cleavage. The dynamics at 332 nm is most interesting (Figure 6e, blue curve), because the ESA decreases within ~30 ps, while the benzhydryl radicals **E12**$^{\bullet}$ appear with a marked delay ($k_{obs} = 3.8 \times 10^9$ s^{-1}). The dent between the decrease of the ESA and the formation of **E12**$^{\bullet}$ implies the accumulation of a "dark" intermediate with a relatively low absorption coefficient which cannot be detected within the large probe range from 290 to 700 nm. This intermediate might be the phosphoranyl/chlorine radical pair [**E12**-$PPh_3^{\bullet}Cl^{\bullet}$] (Scheme 2b, green pathway), which can either dissociate to **E12**$^{\bullet}$ and PPh_3 or undergo a back electron transfer to regenerate the phosphonium chloride **E12**-$PPh_3^+Cl^-$. After ~800 ps, the "dark" intermediate is completely consumed and the formation of **E12**$^{\bullet}$ ceases.

Due to the lower oxidation potential of bromide, electron transfer reactions from Br^-, which generate $Br^{\bullet}$, are more favorable than the corresponding reactions of Cl^-. Thus, the PET pathway yielding the radical **E12**$^{\bullet}$ from the excited state is extremely effective when $X^- = Br^-$. As a result, the ESA disappears almost instantaneously and the band of **E12**$^{\bullet}$ appears within a few ps (Figure 6f). Accordingly, only a very small amount of carbocation **E12**$^+$ is generated from **E12**-$PPh_3^+Br^-$ in CH_2Cl_2; again the decay of **E12**$^+$ is very effective due to combination with Br^-. In contrast to the observations with the chloride precursor, the radical band keeps rising with an observed rate constant of $k_{obs} = 6.3 \times 10^8$ s^{-1} throughout the whole time scale (Figure 6f, blue curve), i.e., the radical formation is slower but more effective in the case of $X^- = Br^-$. This effect is also explained by the lower oxidation potential of Br^-: After formation of the not observable phosphoranyl radical, homolytic cleavage of **E12**-$PPh_3^{\bullet}$ yields $Ph_2CH^{\bullet}$ (green pathway in Scheme 2b). On the other hand, the concurrent back electron transfer depends greatly on the reduction potential of $X^{\bullet}$ and is much less important with $Br^{\bullet}$ than with $Cl^{\bullet}$. As the back electron transfer decay pathway for the "dark" state is suppressed, this state becomes longer-lived and benzhydryl radicals **E12**$^{\bullet}$ keep forming over the whole time scale (Figure 6f) in a more effective and longer-ongoing[51] process. Furthermore, many benzhydryl radicals **E12**$^{\bullet}$ survive due to the less important electron transfer and radical combination reactions between **E12**$^{\bullet}$ and $Br^{\bullet}$.

Ion-Pairing and UV/Vis Spectra of the Photo-generated Benzhydryl Cations. It should be noted that the carbocations E^+ which are obtained by the heterolytic cleavage from the paired precursor salts [**E**-$PR_3^+X^-$] (Scheme 2b, red pathway) may remain paired with the negatively charged counterions during escape of PR_3 from the solvent cage [$E^+PR_3X^-$]. Thus, if the association equilibrium of the benzhydrylium salt E^+X^- is favorable enough and X^- is a weakly nucleophilic counter-ion (e.g., SbF_6^-), photolysis of [**E**-$PR_3^+X^-$] yields long-lived ion pairs [E^+X^-].

Figure 5b shows that the absorption maxima of the carbocations in CH_2Cl_2 vary slightly with the counter-anions. The absorption maxima λ_{max} of the benzhydryl cations **E12**$^+$ which were generated from the phosphonium halide precursors are at slightly higher wavelengths ($\lambda_{max} \approx 450$ nm, Figure 5b, red and green curves) than those of the benzhydrylium ions generated from the phosphonium tetrafluoroborate or hexafluoroantimonate precursors ($\lambda_{max} \approx 443$ and 445 nm, Figure 5b, black and blue curves). It has previously been reported that the absorption maxima of the paired benzhydrylium tetrachloroborates [**E(3–8)**$^+BCl_4^-$] are at ~2 nm shorter wavelengths than those of the free ions.[52] Thus, the lower λ_{max} of the benzhydrylium ions **E12**$^+$ which were generated from BF_4^- or SbF_6^- salts are in agreement with the presence of benzhydrylium ion pairs. The same λ_{max} as shown in Figure 5b (determined with 10 ns gate width) are also observed by the ultrafast measurements after ~1 ns and then remain constant during the whole lifetime (μs time scale) of **E12**$^+$ (see Figure S7 in the Supporting Information). As the diffusional approach of external anions is

comparably slow, the paired benzhydrylium ions observed after ~1 ns must originate from paired phosphonium salts.

The higher λ_{max} for the benzhydryl cations **E12**$^+$ obtained from the halide precursors (Figure 5b, red and green curves) can be explained by the fact that carbocations which originate from the paired fraction of the phosphonium halide precursors are immediately trapped by the halide anions. Thus, the carbocations which we can observe spectrophotometrically on the >10 ns time scale[53] are only the free (unpaired) benzhydrylium ions **E12**$^+$ which are obtained from the unpaired fraction of the phosphonium halides. External halide ions subsequently consume the unpaired benzhydrylium ions in a diffusion-controlled reaction (see below) which does not affect λ_{max} of the remaining unpaired benzhydrylium ions but only reduces the signal intensity.

In CH_3CN, the precursor salts as well as the benzhydryl cations are mostly unpaired in the concentration range employed in our experiments, and we observe the unpaired carbocations **E12**$^+$ predominantly. Thus, the absorption bands of **E12**$^+$ feature identical absorption maxima ($\lambda_{max} \approx 436$ nm) irrespective of the counterions in this solvent (Figure 5a).

Counterion Effects in the Photochemistry of Other Onium Salts. The counterion effects discussed in the preceding paragraphs should also be relevant for the photochemistry of other onium salts. For example, we have previously shown that one can generate **E12**$^+$ in CH_2Cl_2 by laser flash photolysis of the quaternary ammonium tetrafluoroborate **E12**-DABCO$^+$BF$_4^-$ (DABCO = 1,4-diazabicyclo[2.2.2]octane) but not from the corresponding quaternary ammonium bromide.[14] Benzhydryl trimethylammonium iodide has also been used as photo-base-generator because irradiation of **E12**-NMe$_3^+$I$^-$ yields trimethylamine but not the benzhydryl cation **E12**$^+$ which would trap the amine.[22] To account for the formation of NMe_3 and the absence of **E12**$^+$, Jensen and Hanson discarded the PET mechanism and favored a photo-S$_N$1 reaction in CH_3CN and CH_3OH which involves photoheterolysis of the precursor with subsequent trapping of the benzhydryl cations **E12**$^+$ by the I$^-$ anions or the nucleophilic solvent.[22b] Our results with the phosphonium analogues suggest that the PET mechanism may well be a relevant pathway for the generation of tertiary amines in less polar solvents.

3.6. Laser Flash Photolytic Generation of Highly Electrophilic Benzhydrylium Ions. The information on the influence of photo-nucleofuges (PAr_3) and counter-ions X$^-$ on carbocation yields derived in the previous sections have subsequently been used to generate highly reactive carbocations in order to study their reactivities in bimolecular reactions on the >10 ns time scale. For these investigations, we were restricted to the solvent CH_2Cl_2, because CH_3CN reacts fast with highly electrophilic benzhydrylium ions such as **E(14−20)**$^+$ (see below). In section 3.3 we have already demonstrated that the use of P(p-Cl-C$_6$H$_4$)$_3$ as photo-nucleofuge gives higher yields of carbocations than when PPh_3 is employed. Figure 7a shows the transient spectra obtained by irradiating solutions of the phosphonium salts **E18**-P(p-Cl-C$_6$H$_4$)$_3^+$X$^-$ with different counter-anions X$^-$ in CH_2Cl_2 with a 7-ns laser pulse (λ_{exc} = 266 nm). As discussed in section 3.3, the phosphonium tetrafluoroborate **E18**-P(p-Cl-C$_6$H$_4$)$_3^+$BF$_4^-$ gave a moderate yield of **E18**$^+$ along with significant amounts of **E18**$^\bullet$ (Figure 7a, black curve). In view of the results presented in section 3.5 it is no surprise that we could not observe any carbocation **E18**$^+$ but only the radical **E18**$^\bullet$ when we irradiated the phosphonium bromide **E18**-P(p-Cl-C$_6$H$_4$)$_3^+$Br$^-$ (Figure 7a, red curve).

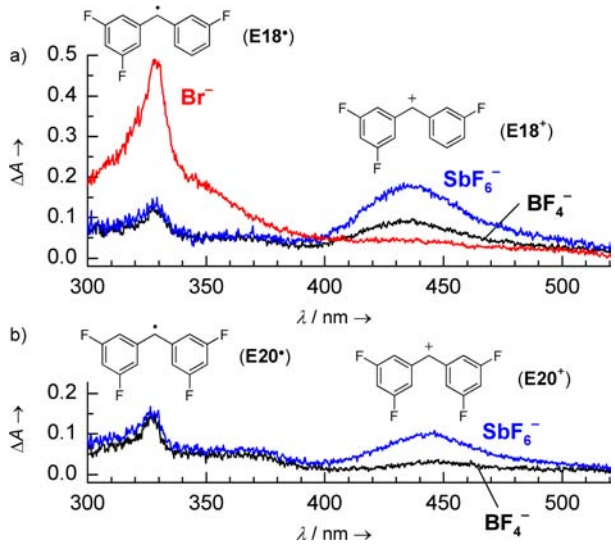

Figure 7. Transient spectra obtained after irradiation of CH_2Cl_2 solutions of benzhydryl tris(p-chlorophenyl)phosphonium salts with different counter-anions with a 7-ns laser pulse (λ_{exc} = 266 nm, gate width: 10 ns): (a) **E18**-P(p-Cl-C$_6$H$_4$)$_3^+$X$^-$ with X$^-$ = BF$_4^-$ (black, $A_{266\,nm}$ = 1.0), X$^-$ = SbF$_6^-$ (blue, $A_{266\,nm}$ = 1.0) and X$^-$ = Br$^-$ (red, $A_{266\,nm}$ = 1.0); (b) **E20**-P(p-Cl-C$_6$H$_4$)$_3^+$X$^-$ with X$^-$ = BF$_4^-$ (black, $A_{266\,nm}$ = 1.0) and X$^-$ = SbF$_6^-$ (blue, $A_{266\,nm}$ = 0.9).

When we irradiated CH_2Cl_2 solutions of the phosphonium hexafluoroantimonate **E18**-P(p-Cl-C$_6$H$_4$)$_3^+$SbF$_6^-$, however, the intensity of the cation band was doubled compared with that obtained from the corresponding BF$_4^-$ salt, while that of the radical band remained virtually unchanged (Figure 7a, blue line).

Similarly, the absorbance of **E20**$^+$ more than tripled when we used the hexafluoroantimonate **E20**-P(p-Cl-C$_6$H$_4$)$_3^+$SbF$_6^-$ (Figure 7b, blue curve) instead of the corresponding tetrafluoroborate (Figure 7b, black curve), while the yield of the benzhydryl radical **E20**$^\bullet$ was unaffected. The combination of the P(p-Cl-C$_6$H$_4$)$_3$ photo-leaving group and the SbF$_6^-$ counter-ion hence finally allowed us to generate **E20**$^+$ in sufficient concentrations to study its kinetics with nucleophiles in CH_2Cl_2. Similarly, we could also obtain the highly electrophilic 4,4′-bis(trifluoromethyl)benzhydrylium ion **E19**$^+$ from **E19**-P(p-Cl-C$_6$H$_4$)$_3^+$SbF$_6^-$ (Figure S8 in the Supporting Information).

Apparently, the BF$_4^-$ anions trap a significant portion of the carbocations **E(18−20)**$^+$ within the [**E**$^+$BF$_4^-$] ion pairs that are generated by the laser pulse. This is not the case for the parent benzhydryl cation **E12**$^+$ which was obtained in similar concentrations from the hexafluoroantimonate and the tetrafluoroborate precursor (Figure 5b, black and blue curves); on the microsecond time scale we also see a faster decay with the BF$_4^-$ counterion than with SbF$_6^-$ (see below). The trapping of the carbocation by BF$_4^-$ within the ion pair becomes less efficient as the electrophilicity of the carbocations is reduced. The higher reactivity of BF$_4^-$ compared to SbF$_6^-$ is in agreement with the calculated enthalpies of fluoride abstractions in the gas phase, which are 151 kJ mol^{-1} more exothermic for BF$_4^-$ than for SbF$_6^-$.[54] Furthermore, the photoinitiation efficiencies of onium salts in cationic polymerizations generally depend on the nature of the anions and decrease in the order SbF$_6^-$ > AsF$_6^-$ > PF$_6^-$ > BF$_4^-$.[26] This is usually explained by the different nucleophilicities of the anions which are considered to be relevant for the stability of the active center in the propagation step of cationic polymerizations.[26]

3.7. Lifetimes of Benzhydrylium Ions in CH_2Cl_2, CH_3CN, and CF_3CH_2OH. Not only the yields of the carbocations $\mathbf{E}^+$ on the ≤10 ns time scale but also their lifetimes on the μs time scale depend greatly on the experimental conditions. Figure 8 shows

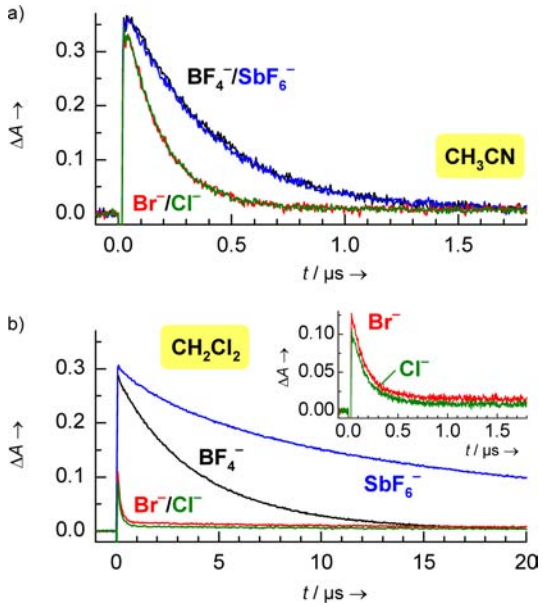

Figure 8. Time-dependent absorbances of $\mathbf{E12}^+$ obtained after 7-ns irradiation of $\mathbf{E12}$-$PPh_3^+X^-$ ($A_{266\,nm}$ = 0.5, (1.0−1.2) × 10^{-4} M) with different counter-anions X^- = BF_4^- (black), SbF_6^- (blue), Br^- (red) or Cl^- (green) with a 7-ns laser pulse: (a) in CH_3CN and (b) in CH_2Cl_2 (inset: enlarged decay curves for $\mathbf{E12}^+$ from precursors with halide counterions).

the time-dependent absorbances of the parent benzhydrylium ion $\mathbf{E12}^+$, which we observed when we generated this carbocation from precursors $\mathbf{E12}$-$PPh_3^+X^-$ with different counter-anions (X^- = BF_4^-, SbF_6^-, Br^-, or Cl^-) in CH_3CN or CH_2Cl_2. The lifetime of $\mathbf{E12}^+$ depends on the decay mechanism of the carbocation, which can be (i) recombination with the photo-leaving group PPh_3, (ii) reaction with the counter-anions X^- of the phosphonium salt precursor, or (iii) reaction with the solvent.

Recombination with the Photo-nucleofuge. A general limitation of the laser flash photolysis technique is entailed by the recombination reactions of the carbocations with the free (diffusionally separated) photo-nucleofuges. Photo-nucleofuges (e.g., Hal^-, NR_3, PR_3, RCO_2^-) typically undergo diffusion-controlled recombination reactions with highly electrophilic carbocations (E > 0) in solvents of low nucleophilicity.[55] Exceptions to this rule are anionic photo-leaving groups in fluorinated alcohols which stabilize anions very well (e.g., acetate or *p*-cyanophenolate in CF_3CH_2OH).[8] In our case, the triarylphosphines (N ≥ 12.58, s_N = 0.65)[37] undergo diffusion-controlled or almost diffusion-controlled reactions with the benzhydrylium ions $\mathbf{E(1-20)}^+$.

The blue curve in Figure 8b shows that the recombination reaction with PPh_3 can be observed when $\mathbf{E12}^+$ is generated by irradiation of $\mathbf{E12}$-$PPh_3^+SbF_6^-$ in CH_2Cl_2. Since $\mathbf{E12}^+$ and PPh_3 are generated in equimolar amounts by the laser pulse, the observed decay of the absorbance is not mono-exponential. Using the software Gepasi,[43] we could fit the observed decay to a kinetic model which takes into account the second-order recombination reaction with PPh_3 and a general first-order reaction which summarizes all (pseudo-)first-order reactions which may occur (Figure 9). Details and more examples of such

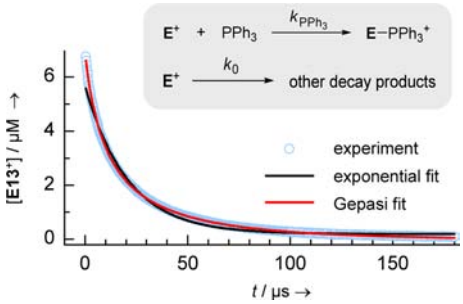

Figure 9. Decay of the concentration of $\mathbf{E12}^+$ observed after irradiation of $\mathbf{E12}$-$PPh_3^+SbF_6^-$ ($A_{266\,nm}$ = 0.53, 1.03 × 10^{-4} M) in CH_2Cl_2 with a 7-ns laser pulse: Superposition of experimental data (○), an exponential fit (black), and a fit calculated by Gepasi (red) according to the kinetic model with variable [PPh_3] shown in this Figure (k_{PPh_3} = (1.31 ± 0.003) × 10^{10} M^{-1} s^{-1} and k_0 = (6.49 ± 0.02) × 10^3 s^{-1}).

fits can be found in section S9 of the Supporting Information. As expected, second-order rate constants k_{PPh_3} ≈ 1 × 10^{10} M^{-1} s^{-1} are found for the combinations of $\mathbf{E8}^+$, $\mathbf{E9}^+$, and $\mathbf{E12}^+$ with PPh_3, indicating diffusion-controlled reactions. The obtained rate constants k_0 (s^{-1}) for the first-order background decay reactions agree with the trends discussed below.

At typical concentrations of the photofragments $\mathbf{E}^+$ and PAr_3 in our experiments (∼10^{-6}−10^{-5} M), we find such non-exponential decay kinetics for all systems in which the benzhydryl cations $\mathbf{E}^+$ have lifetimes >10 μs. The recombination reaction with the photo-leaving group thus sets a lower limit for measuring pseudo-first-order kinetics of the benzhydryl cations $\mathbf{E}^+$ with external nucleophiles: Only pseudo-first-order rate constants larger than (1−5) × 10^5 s^{-1} can be determined reliably by fitting the data to an exponential decay curve; otherwise the decay kinetics will be dominated by the second-order reaction with the photo-leaving group.

Reaction with the Counter-anion of the Precursor Phosphonium Salt. When precursors $\mathbf{E}$-$PPh_3^+X^-$ with halide counter-anions were used for the generation of benzhydryl cations $\mathbf{E}^+$, we observed exponential decays of the carbocations which were significantly faster than the decays of carbocations generated from phosphonium salts with X^- = BF_4^- or SbF_6^- (Figure 8). Halide ions undergo diffusion-controlled reactions with reactive carbocations (E > −2) in aprotic solvents[7] and the reactions follow pseudo-first-order kinetics since [$\mathbf{E}^+$] ≪ [X^-] (only a small fraction of Ar_2CH-$PPh_3^+X^-$ is cleaved to the carbocations). For example, irradiation of 1.2 × 10^{-4} M solutions of $\mathbf{E12}$-$PPh_3^+X^-$ with X^- = Br^- or Cl^- in CH_3CN (Figure 8a, red and green curves) gave pseudo-first-order rate constants k_{obs} ≈ 6 × 10^6 s^{-1} for the decay of $\mathbf{E12}^+$. Irradiation of 1.0 × 10^{-4} M solutions of the same precursors in CH_2Cl_2 (Figure 8b, red and green curves) yielded similar rate constants (k_{obs} ≈ 7 × 10^6 s^{-1}). These values correspond to second-order rate constants of k_2 ≈ 5 × 10^{10} M^{-1} s^{-1} (CH_3CN) and k_2 ≈ 7 × 10^{10} M^{-1} s^{-1} (CH_2Cl_2) for the diffusion-controlled reactions of $\mathbf{E12}^+$ with Br^- and Cl^-.

An almost mono-exponential decay of $\mathbf{E12}^+$ was also observed in CH_2Cl_2 when we irradiated $\mathbf{E12}$-$PPh_3^+X^-$ with X^- = BF_4^- (Figure 8b, black curve, k_{obs} ≈ 2.6 × 10^5 s^{-1}). This decay is much slower than the decays for X^- = Cl^- or Br^- but significantly faster than the non-exponential decay observed for X^- = SbF_6^- (Figure 8b, blue curve) indicating that $\mathbf{E12}^+$ reacts with BF_4^-. Similar

mono-exponential decays were found for the benzhydrylium ions **E(10−17)**$^+$ which were generated from the phosphonium tetrafluoroborates **E(10−17)**-PAr$_3^+$BF$_4^-$; the decay rate constants increase with the electrophilicities E of the carbocations (see section S10 in the Supporting Information for details). As the yields of the more reactive benzhydryl cations **E(18−20)**$^+$ obtained from the BF$_4^-$ salt precursors were lower than those from the SbF$_6^-$ salt precursors (see above), one can conclude that the reactions of **E(18−20)**$^+$ with BF$_4^-$ already occur on time scales <10 ns. For the highly reactive carbocations **E(18−20)**$^+$ we also observed mono-exponential decays when they were generated from the corresponding hexafluoroantimonate salts **E(18−20)**-P(p-Cl-C$_6$H$_4$)$_3^+$SbF$_6^-$. As the background decay rates k_0 of the carbocations **E(18−20)**$^+$ observed on the >10 ns time scale after irradiation of **E(18−20)**-P(p-Cl-C$_6$H$_4$)$_3^+$X$^-$ with X$^-$ = BF$_4^-$ and SbF$_6^-$ also become similar (Figure S10.2 in the Supporting Information), we assume that now the reactions of **E**$^+$ with solvent impurities such as residual water in CH$_2$Cl$_2$ are dominating.

We have already discussed in section 3.5 that the benzhydrylium tetrafluoroborates **E**$^+$BF$_4^-$ predominantly exist as ion pairs in CH$_2$Cl$_2$ solutions (in the presence of ~1 × 10^{-4} M phosphonium tetrafluoroborate). Accordingly, a further increase of the concentration of BF$_4^-$ has little effect on the kinetics. Thus, the decay rate constant of **E18**$^+$ increased only slightly (factor 1.5) when we irradiated CH$_2$Cl$_2$ solutions of **E18**-P(p-Cl-C$_6$H$_4$)$_3^+$BF$_4^-$ in the presence of 1.4 × 10^{-2} M KBF$_4$/18-crown-6. The high concentration of BF$_4^-$ ions reduced the initial absorbance of **E18**$^+$ by less than 30%, i.e., the effect is much smaller than when exchanging 5.7 × 10^{-5} M SbF$_6^-$ for the same concentration of BF$_4^-$ (Figure 7a).

Reactions with the Solvent. In CH$_3$CN or 2,2,2-trifluoroethanol (TFE), which are typical solvents for the laser-flash-photolytic generation of carbocations,[1] the characterization of highly electrophilic carbocations is hampered by the nucleophilicity of these solvents. In CH$_3$CN, for example, the parent benzhydryl cation **E12**$^+$ decays mono-exponentially with a first-order rate constant of k_1 = 2.52 × 10^6 s^{-1} when it is generated from **E12**-PPh$_3^+$BF$_4^-$ or SbF$_6^-$ (Figure 8a), that is, it decays at least 1 order of magnitude faster than in CH$_2$Cl$_2$. A slightly larger value (k_1 = 3.21 × 10^6 s^{-1}) was observed for the decay of **E12**$^+$ in trifluoroethanol (TFE). These rate constants are independent of the choice of the photo-leaving groups (Table 3). As solvation effects have a relatively small influence on the reactivities of carbocations,[56] the ~440-fold increase of the decay rate of **E12**$^+$ in CH$_3$CN and TFE compared with CH$_2$Cl$_2$ (k_0 ≈ 6.5 × 10^3 s^{-1}, Figure 9) must result from reactions of **E12**$^+$ with these solvents.[8,9,40]

The most reactive benzhydryl cations of this series, **E18**$^+$, **E19**$^+$, and **E20**$^+$, decay too fast in CH$_3$CN or TFE (τ < 10 ns) to be observed with the nanosecond laser flash photolysis setup. It is possible, however, to generate the acceptor-substituted benzhydrylium ions **E(14−17)**$^+$ in these solvents and to follow the exponential decays of their UV/vis absorbances. Since the first-order rate constants for their reactions with CH$_3$CN and TFE are ≥1 × 10^7 s^{-1} (Table 3), it is difficult to characterize the electrophilic reactivities of these benzhydrylium ions toward other nucleophiles in these solvents, because only nucleophiles that react with rate constants close to the diffusion limit can efficiently compete with these solvents.

Dichloromethane is considerably less nucleophilic than CH$_3$CN or TFE. First-order decay rate constants of ~2 × 10^6 s^{-1} (**E18**$^+$) and ~3 × 10^6 s^{-1} (**E20**$^+$) were measured when these carbocations were generated from **E(18,20)**-P(p-Cl-C$_6$H$_4$)$_3^+$SbF$_6^-$ (Figure S10.2 in the Supporting Information). However, these values are probably due to impurities and do not reflect the reactivity of CH$_2$Cl$_2$ (see above). They just represent an upper limit for the nucleophilic reactivity of CH$_2$Cl$_2$. Anyway, the lifetimes of the benzhydrylium ions in highly purified CH$_2$Cl$_2$ (see Experimental Section) are much longer than in anhydrous CH$_3$CN and TFE and allow us to study the electrophilic reactivities of **E(14−20)**$^+$ toward a variety of nucleophiles.

Table 3. First-Order Rate Constants k_1 (s^{-1}) for the Decay of Benzhydryl Cations E$^+$ in CH$_3$CN and 2,2,2-Trifluoroethanol (TFE) at 20 °C

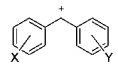

E$^+$	X	Y	E[a]	k_1 (CH$_3$CN) / s^{-1}	k_1 (TFE) / s^{-1}
E10$^+$	4-F	4-F	5.01	1.1 × 10^6 [b]	5.82 × 10^5 [c]
E11$^+$	4-F	H	5.20	1.8 × 10^6 [b]	[d]
E12$^+$	H	H	5.47	2.52 × 10^6 [c,e]	3.21 × 10^6 [c,f]
E13$^+$	4-Cl	4-Cl	5.48	2.8 × 10^6 [b]	1.47 × 10^6 [c]
E14$^+$	3-F	H	6.23	1.00 × 10^7 [c]	1.29 × 10^7 [c]
E15$^+$	4-(CF$_3$)	H	6.70	3.8 × 10^7 [b]	[d]
E17$^+$	3-F	3-F	6.87	3.49 × 10^7 [c]	4.6 × 10^7 [c]

[a]Electrophilicity parameters E of the benzhydryl cations **E**$^+$; see Table 1 for references. [b]Photolysis of **E**-Cl in CH$_3$CN.[40] [c]Photolysis of **E**-PPh$_3^+$BF$_4^-$, this work. [d]Not determined. [e]Photolysis of **E12**-Cl in CH$_3$CN gave a value of 2.5 × 10^6 s^{-1}.[40] [f]Photolysis of benzhydryl p-cyanophenyl ether in TFE gave a value of 3.2 × 10^6 s^{-1}.[8]

3.8. Counter-ion Effects on Bimolecular Reactions. As discussed in section 3.5, the usual assumption that only free ions are observed in nanosecond laser flash photolysis experiments[1a,b] does not hold when the carbocations are generated by photolysis of certain onium salts with low-nucleophilicity counter-ions (e.g., BF$_4^-$, SbF$_6^-$). Consequently, the question arises whether bimolecular reactions of the photolytically generated carbocations are affected by the nature of the counter-anion in the precursor salt. Previous results already showed that the rate constants for the reactions of moderately stabilized benzhydrylium ions such as methoxy- or methyl substituted benzhydrylium ions **E(3−9)**$^+$ with neutral nucleophiles like π-nucleophiles[3d,56,57] or hydride donors[58] in CH$_2$Cl$_2$ are independent of the nature of the counter-anion and the degree of ion pairing. We now investigated the influence of the counter-anion on the reactions of the considerably more electrophilic benzhydrylium ions **E12**$^+$ and **E18**$^+$ with π-nucleophiles (Table 4).

When we generated the benzhydrylium ions **E**$^+$ from different precursors **E**-PAr$_3^+$X$^-$ with different counter-anions X$^-$ in the presence of a large excess of π-nucleophiles, we observed exponential decays of the UV/vis absorbances of the benzhydryl cations **E**$^+$ from which we obtained the pseudo-first-order rate constants k_{obs} (s^{-1}). Plots of k_{obs} versus the nucleophile concentrations were linear in all cases, as exemplified in Figure 10 for the reaction of **E12**$^+$ with allyltrimethylsilane.

The intercepts of these plots vary with the counter-anion X$^-$ of the phosphonium salts and correspond to the rate constants k_0 for the background decay reactions discussed in section 3.7. For X$^-$ = Br$^-$ and Cl$^-$, we find quite large intercepts of k_0 ≈ 7 × 10^6 s^{-1} due to the diffusion-controlled reactions of **E**$^+$ with the halide anions. For X$^-$ = BF$_4^-$ and SbF$_6^-$, the intercepts are substantially

Table 4. Second-Order Rate Constants k_2 (M^{-1} s^{-1}) for the Reactions of π-Nucleophiles with Benzhydryl Cations E^+ Obtained from Different Precursors E-$PAr_3^+X^-$ in CH_2Cl_2 at 20 °C

	precursor E-$PAr_3^+X^-$		
E^+	PAr_3	X^-	k_2/M^{-1} s^{-1}
E12$^+$	Reaction with allyltrimethylsilane		
	PPh_3	BF_4^-	1.60×10^7
	PPh_3	SbF_6^-	1.43×10^7
	PPh_3	Br^-	1.42×10^7
	PPh_3	Cl^-	1.53×10^7
E18$^+$	Reaction with 2,3-dimethyl-1-butene		
	PPh_3	BF_4^-	8.22×10^7
	$P(p\text{-Cl-}C_6H_4)_3$	BF_4^-	8.24×10^7
	$P(p\text{-Cl-}C_6H_4)_3$	SbF_6^-	8.27×10^7

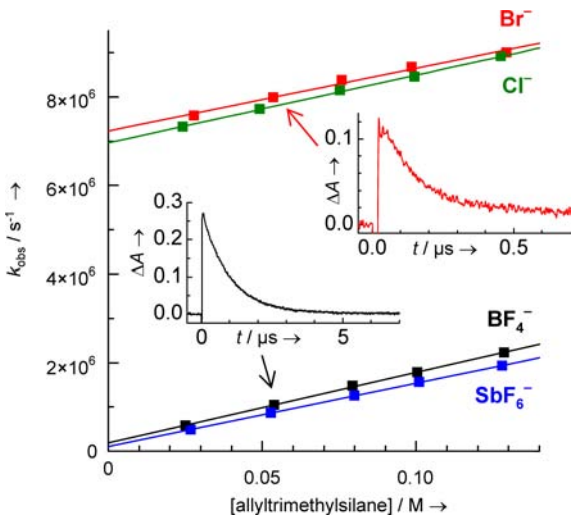

Figure 10. Plots of the pseudo-first-order rate constants k_{obs} (s^{-1}) for the reactions of **E12**$^+$ with allyltrimethylsilane in CH_2Cl_2 when **E12**$^+$ was generated by irradiation of 1.0×10^{-4} M solutions of the precursors **E12**-PPh_3X^- with different counter-anions $X^- = BF_4^-$ (black squares), SbF_6^- (blue squares), Br^- (red squares), or Cl^- (green squares) against the concentration of allyltrimethylsilane. The small graphs show the absorbance decays of **E12**$^+$ in presence of 5.4×10^{-2} M allyltrimethylsilane (black curve, $X^- = BF_4^-$; red curve, $X^- = Br^-$).

lower and their origin has been discussed above. The slopes of the four plots are independent of the counter-anion and provide the second-order rate constants k_2 (M^{-1} s^{-1}) for the reaction of **E12**$^+$ with allyltrimethylsilane listed in Table 4. We thus measured the same rate constants within experimental error for the reactions of **E12**$^+$ with allyltrimethylsilane when **E12**$^+$ was generated from different precursors **E12**-$PPh_3^+X^-$ with X^- = BF_4^-, SbF_6^-, Br^-, or Cl^- (Table 4). As discussed in section 3.5, the benzhydryl cations obtained from precursors with halide ions are the free (unpaired) cations because [**E12**$^+$ Hal^-] pairs collapse to covalent **E12**-Hal in less than 10 ns. Since **E12**$^+BF_4^-$ and **E12**$^+SbF_6^-$ are significantly paired, on the other hand, we can conclude that paired and unpaired benzhydrylium ions **E12**$^+$ react with the same rate constants in bimolecular reactions and can be characterized by an anion-independent electrophilicity parameter (E = 5.47).

The same situation has been observed for the reactions of 2,3-dimethyl-1-butene with **E18**$^+$, which is the most electrophilic carbocation (E = 7.52) in our series that could be obtained from precursors with different counterions. When we generated **E18**$^+$ from either **E18**-$P(p\text{-Cl-}C_6H_4)_3^+BF_4^-$ or **E18**-$P(p\text{-Cl-}C_6H_4)_3^+SbF_6^-$, we again measured the same rate constants within experimental error (Table 4). Moreover, we also obtained the same rate constant when we used **E18**-$PPh_3^+BF_4^-$ as precursor, which shows that the photo-leaving group does not have any effect on the carbocations' reactivities either. As discussed in section 3.6, we could not generate **E18**$^+$ from the phosphonium bromide precursor in CH_2Cl_2 (radical formation), and therefore we cannot compare the reactivities of free and paired carbocations in this case. The counterion independence of the experimental rate constants for carbocation alkene combination reactions implies that ion pairing stabilizes the transition states to about the same extent as the reactant carbocations.

4. CONCLUSION

The efficiencies of the photo-generation of benzhydrylium ions and benzhydryl radicals from phosphonium salts E-$PAr_3^+X^-$ depend not only on the photo-electrofuge (E^+) and the photo-leaving group PAr_3, but also on the counter-ion X^-, the solvent, and the concentration of the precursor molecules. Depending on the reaction conditions, benzhydryl radicals $E^\bullet$ or benzhydryl cations E^+ may be obtained almost exclusively. The results presented in this work should also be relevant for the photochemistry of other onium salts. Spectroscopic investigations on the fs to ps time scale like those performed in this and related work[4,5,16,45] provide a complete microscopic understanding of the photo-generation and the dynamics of reactive intermediates in the geminate solvent cage. With the knowledge of phosphonium salt photochemistry acquired from the present study, we can now select the proper precursor salts for the efficient generation of highly reactive carbocations which are not easily accessible by conventional methods. The method described in this work will subsequently be used to characterize the electrophilic reactivities of the acceptor-substituted benzhydrylium ions **E(14−20)**$^+$ in CH_2Cl_2 at 20 °C, which provides a further extension of our long-ranging electrophilicity scale.[41]

■ ASSOCIATED CONTENT

Supporting Information

Additional transient spectra, details of the experimental procedures and data evaluation, details of the kinetic measurements. This material is available free of charge via the Internet at http://pubs.acs.org.

■ AUTHOR INFORMATION

Corresponding Author

Herbert.Mayr@cup.uni-muenchen.de

Notes

The authors declare no competing financial interest.

■ ACKNOWLEDGMENTS

We thank Prof. Shinjiro Kobayashi for setting up the nanosecond laser flash working station, Dr. Armin Ofial, Dr. Igor Pugliesi, Sebastian Thallmair, and Konstantin Troshin for helpful discussions, Christoph Grill for early experimental work, and the Deutsche Forschungsgemeinschaft (SFB 749) for financial support.

REFERENCES

(1) Reviews: (a) McClelland, R. A. In *Reactive Intermediate Chemistry*; Moss, R. A., Platz, M. S., Jones, M. J., Eds.; Wiley: Hoboken, NJ, 2004, p 3−40. (b) McClelland, R. A. *Tetrahedron* **1996**, *52*, 6823−6858. (c) Fleming, S. A.; Pincock, J. A. *Mol. Supramol. Photochem.* **1999**, *3*, 211−281. (d) Das, P. K. *Chem. Rev.* **1993**, *93*, 119−144.

(2) McClelland, R. A.; Chan, C.; Cozens, F. L.; Modro, A.; Steenken, S. *Angew. Chem.* **1991**, *103*, 1389−1391; *Angew. Chem., Int. Ed.* **1991**, *30*, 1337−1339.

(3) (a) Bartl, J.; Steenken, S.; Mayr, H. *J. Am. Chem. Soc.* **1991**, *113*, 7710−7716. (b) Johnston, L. J.; Kwong, P.; Shelemay, A.; Lee-Ruff, E. *J. Am. Chem. Soc.* **1993**, *115*, 1664−1669. (c) Kobayashi, S.; Hori, Y.; Hasako, T.; Koga, K.-i.; Yamataka, H. *J. Org. Chem.* **1996**, *61*, 5274−5279. (d) Mayr, H.; Schimmel, H.; Kobayashi, S.; Kotani, M.; Prabakaran, T. R.; Sipos, L.; Faust, R. *Macromolecules* **2002**, *35*, 4611−4615. (e) Phan, B. T.; Nolte, C.; Kobayashi, S.; Ofial, A. R.; Mayr, H. *J. Am. Chem. Soc.* **2009**, *131*, 11392−11401.

(4) Sailer, C. F.; Fingerhut, B. P.; Thallmair, S.; Nolte, C.; Ammer, J.; Mayr, H.; de Vivie-Riedle, R.; Pugliesi, I.; Riedle, E. *J. Am. Chem. Soc.* **2012**, submitted.

(5) Sailer, C. F.; Fingerhut, B. P.; Ammer, J.; Nolte, C.; Pugliesi, I.; Mayr, H.; de Vivie-Riedle, R.; Riedle, E. In *Ultrafast Phenomena XVII*; Chergui, M., Jonas, D., Riedle, E., Schoenlein, R. W., Taylor, A., Eds.; Oxford University Press: New York, 2011; pp 427−429.

(6) (a) McClelland, R. A.; Banait, N.; Steenken, S. *J. Am. Chem. Soc.* **1986**, *108*, 7023−7027. (b) McClelland, R. A.; Kanagasabapathy, V. M.; Banait, N. S.; Steenken, S. *J. Am. Chem. Soc.* **1989**, *111*, 3966−3972. (c) McClelland, R. A.; Kanagasabapathy, V. M.; Banait, N. S.; Steenken, S. *J. Am. Chem. Soc.* **1991**, *113*, 1009−1014. (d) McClelland, R. A.; Kanagasabapathy, V. M.; Banait, N.; Steenken, S. *J. Am. Chem. Soc.* **1992**, *114*, 1816−1823. (e) Van Pham, T.; McClelland, R. A. *Can. J. Chem.* **2001**, *79*, 1887−1897.

(7) Minegishi, S.; Loos, R.; Kobayashi, S.; Mayr, H. *J. Am. Chem. Soc.* **2005**, *127*, 2641−2649.

(8) McClelland, R. A.; Kanagasabapathy, V. M.; Steenken, S. *J. Am. Chem. Soc.* **1988**, *110*, 6913−6914.

(9) Minegishi, S.; Kobayashi, S.; Mayr, H. *J. Am. Chem. Soc.* **2004**, *126*, 5174−5181.

(10) (a) Hallett-Tapley, G.; Cozens, F. L.; Schepp, N. P. *J. Phys. Org. Chem.* **2009**, *22*, 343−348. (b) Horn, M.; Mayr, H. *Chem.—Eur. J.* **2010**, *16*, 7478−7487. (c) Horn, M.; Mayr, H. *Eur. J. Org. Chem.* **2011**, 6470−6475.

(11) Baidya, M.; Kobayashi, S.; Brotzel, F.; Schmidhammer, U.; Riedle, E.; Mayr, H. *Angew. Chem.* **2007**, *119*, 6288−6292; *Angew. Chem., Int. Ed.* **2007**, *46*, 6176−6179.

(12) (a) Cozens, F.; Li, J.; McClelland, R. A.; Steenken, S. *Angew. Chem.* **1992**, *104*, 753−755; *Angew. Chem., Int. Ed.* **1992**, *31*, 743−745. (b) Mladenova, G.; Chen, L.; Rodriquez, C. F.; Siu, K. W. M.; Johnston, L. J.; Hopkinson, A. C.; Lee-Ruff, E. *J. Org. Chem.* **2001**, *66*, 1109−1114. (c) Loos, R.; Kobayashi, S.; Mayr, H. *J. Am. Chem. Soc.* **2003**, *125*, 14126−14132. (d) Schaller, H. F.; Schmidhammer, U.; Riedle, E.; Mayr, H. *Chem.—Eur. J.* **2008**, *14*, 3866−3868.

(13) See refs 14−18 for kinetic studies using quaternary triarylphosphonium salts and refs 18 and 19 for kinetic studies with other quaternary phosphonium salts as precursors.

(14) Ammer, J.; Baidya, M.; Kobayashi, S.; Mayr, H. *J. Phys. Org. Chem.* **2010**, *23*, 1029−1035.

(15) Ammer, J.; Mayr, H. *Macromolecules* **2010**, *43*, 1719−1723.

(16) Sailer, C. F.; Singh, R. B.; Ammer, J.; Riedle, E.; Pugliesi, I. *Chem. Phys. Lett.* **2011**, *512*, 60−65.

(17) (a) Shi, L.; Horn, M.; Kobayashi, S.; Mayr, H. *Chem.—Eur. J.* **2009**, *15*, 8533−8541. (b) Troshin, K.; Schindele, C.; Mayr, H. *J. Org. Chem.* **2011**, *76*, 9391−9408.

(18) (a) Baidya, M.; Kobayashi, S.; Mayr, H. *J. Am. Chem. Soc.* **2010**, *132*, 4796−4805. (b) Duan, X.-H.; Maji, B.; Mayr, H. *Org. Biomol. Chem.* **2011**, *9*, 8046−8050. (c) Nigst, T. A.; Ammer, J.; Mayr, H. *Angew. Chem.* **2011**, *124*, 1381−1385; *Angew. Chem., Int. Ed.* **2011**, *51*, 1353−1356. (d) Nolte, C.; Ammer, J.; Mayr, H. *J. Org. Chem.* **2012**, *77*, 3325−3335.

(19) (a) Kanzian, T.; Lakhdar, S.; Mayr, H. *Angew. Chem.* **2010**, *121*, 9717−9720; *Angew. Chem., Int. Ed.* **2010**, *49*, 9526−9529. (b) Streidl, N.; Branzan, R.; Mayr, H. *Eur. J. Org. Chem.* **2010**, 4205−4210. (c) Lakhdar, S.; Ammer, J.; Mayr, H. *Angew. Chem.* **2011**, *123*, 10127−10130; *Angew. Chem., Int. Ed.* **2011**, *50*, 9953−9956.

(20) For examples of carbocations generated by photolysis of phosphonium precursors acting as initiating species in carbocationic polymerizations, see: (a) Takata, T.; Takuma, K.; Endo, T. *Makromol. Chem., Rapid Commun.* **1993**, *14*, 203−206. (b) Takuma, K.; Takata, T.; Endo, T. *J. Photopolym. Sci. Technol.* **1993**, *6*, 67−74.

(21) Examples of photoacid generation mechanisms with heterolytic cleavage of carbon−heteroatom bonds: (a) Pohlers, G.; Scaiano, J. C.; Step, E.; Sinta, R. *J. Am. Chem. Soc.* **1999**, *121*, 6167−6175. (b) Sanrame, C. N.; Brandao, M. S. B.; Coenjarts, C.; Scaiano, J. C.; Pohlers, G.; Suzuki, Y.; Cameron, J. F. *Photochem. Photobiol. Sci.* **2004**, *3*, 1052−1057.

(22) Examples for the photogeneration of tertiary amines from benzhydryl derivatives: (a) Hanson, J. E.; Jensen, K. H.; Gargiuolo, N.; Motta, D.; Pingor, D. A.; Novembre, A. E.; Mixon, D. A.; Kometani, J. M.; Knurek, C. In *Microelectronics Technology. Polymers for Advanced Imaging and Packaging*; Reichmanis, E., Ober, C. K., MacDonald, S. A., Iwayanagi, T., Nishikubo, T., Eds.; ACS Symposium Series *614*; American Chemical Society: Washington, DC, 1995. (b) Jensen, K. H.; Hanson, J. E. *Chem. Mater.* **2002**, *14*, 918−923.

(23) Examples for the photogeneration of PPh_3 from quaternary phosphonium salts: (a) Önen, A.; Arsu, N.; Yagci, Y. *Angew. Makromol. Chem.* **1999**, *264*, 56−59. (b) Kasapoglu, F.; Aydin, M.; Arsu, N.; Yagci, Y. *J. Photochem. Photobiol., A* **2003**, *159*, 151−159.

(24) For reviews about photoinitiators, see refs 25 and 26 and the following: (a) Yagci, Y.; Reetz, I. *Prog. Polym. Sci.* **1998**, *23*, 1485−1538. (b) Yagci, Y.; Durmaz, Y. Y.; Aydogan, B. *Chem. Rec.* **2007**, *7*, 78−90. (c) Allonas, X.; Croutxé-Barghorn, C.; Fouassier, J.-P.; Lalevée, J.; Malval, J.-P.; Morlet-Savary, F. In *Lasers in Chemistry*; Lackner, M., Ed.; Wiley-VCH: Weinheim, 2008; Vol. *2*, pp 1001−1027. (d) Suyama, K.; Shirai, M. *Prog. Polym. Sci.* **2009**, *34*, 194−209. (e) Yagci, Y.; Jockusch, S.; Turro, N., J. *Macromolecules* **2010**, *43*, 6245−6260.

(25) (a) Toba, Y. *J. Photopolym. Sci. Technol.* **2003**, *16*, 115−118. (b) Crivello, J. V. *J. Photopolym. Sci. Technol.* **2008**, *21*, 493−497.

(26) (a) Fouassier, J.-P. In *Photoinitiation, Photopolymerization, and Photocuring: Fundamentals and Applications*; Hanser: Munich, 1995; pp 102−144. (b) Lazauskaite, R.; Grazulevicius, J. V. In *Handbook of Photochemistry and Photobiology*; Nalwa, H. S., Ed.; American Scientific Publishers: Stevenson Ranch, CA, 2003; Vol. *2*, pp 335−392.

(27) (a) Miranda, M. A.; Pérez-Prieto, J.; Font-Sanchis, E.; Scaiano, J. C. *Acc. Chem. Res.* **2001**, *34*, 717−726. (b) Kropp, P. J. In *CRC Handbook of Organic Photochemistry and Photobiology*, 2nd ed.; Horspool, W., Lenci, F., Eds.; CRC Press: Boca Raton, 2004; pp 1-1−1-32. (c) Kitamura, T. In *CRC Handbook of Organic Photochemistry and Photobiology*, 2nd ed.; Horspool, W., Lenci, F., Eds.; CRC Press: Boca Raton, 2004; pp 11-1−11-10. (d) Peters, K. S. *Chem. Rev.* **2007**, *107*, 859−873.

(28) Pincock, J. A. *Acc. Chem. Res.* **1997**, *30*, 43−49.

(29) Dektar, J. L.; Hacker, N. P. *J. Org. Chem.* **1991**, *56*, 1838−1844.

(30) Dektar, J. L.; Hacker, N. P. *J. Am. Chem. Soc.* **1990**, *112*, 6004−6015.

(31) Appleton, D. C.; Bull, D. C.; Givens, R. S.; Lillis, V.; McKenna, J.; McKenna, J. M.; Thackeray, S.; Walley, A. R. *J. Chem. Soc., Perkin Trans. 2* **1980**, 77−82.

(32) Imrie, C.; Modro, T. A.; Rohwer, E. R.; Wagener, C. C. P. *J. Org. Chem.* **1993**, *58*, 5643−5649.

(33) Alonso, E. O.; Johnston, L. J.; Scaiano, J. C.; Toscano, V. G. *Can. J. Chem.* **1992**, *70*, 1784−1794.

(34) (a) Alonso, E. O.; Johnston, L. J.; Scaiano, J. C.; Toscano, V. G. *J. Am. Chem. Soc.* **1990**, *112*, 1270−1271. (b) Imrie, C.; Modro, T. A.; Wagener, C. C. P. *J. Chem. Soc., Perkin Trans. 2* **1994**, 1379−1382.

(35) For general reviews, see refs 1 and 26. Similar photocleavage mechanisms were previously discussed for halides (refs 4 and 27), carboxylates (ref 28), halonium salts (ref 29), sulfonium salts (ref 30), ammonium salts (ref 31), and phosphonium salts (refs 32 and 33).

(36) For equilibrium constants of stabilized benzhydryl cations with triarylphosphines, see ref 37. In cases where highly stabilized carbocations do not give stable triarylphosphonium salts, one may use a more Lewis-basic phosphine such as $P(n\text{-Bu})_3$ as the photo-leaving group (refs 18 and 19).
(37) Kempf, B.; Mayr, H. *Chem.—Eur. J.* **2005**, *11*, 917−927.
(38) For a review of the literature up to 1994, see: Dankowski, M. In *The chemistry of organophosphorus compounds*; Hartley, F. R., Ed.; Wiley: Chichester, 1994; Vol. 3, pp 325−343.
(39) Megerle, U.; Pugliesi, I.; Schriever, C.; Sailer, C. F.; Riedle, E. *Appl. Phys. B: Laser Opt.* **2009**, *96*, 215−231.
(40) Bartl, J.; Steenken, S.; Mayr, H.; McClelland, R. A. *J. Am. Chem. Soc.* **1990**, *112*, 6918−6928.
(41) (a) Mayr, H.; Bug, T.; Gotta, M. F.; Hering, N.; Irrgang, B.; Janker, B.; Kempf, B.; Loos, R.; Ofial, A. R.; Remennikov, G.; Schimmel, H. *J. Am. Chem. Soc.* **2001**, *123*, 9500−9512. (b) Mayr, H.; Kempf, B.; Ofial, A. R. *Acc. Chem. Res.* **2003**, *36*, 66−77. (c) For a comprehensive database of nucleophilicity and electrophilicity parameters, see: http://www.cup.lmu.de/oc/mayr/DBintro.html.
(42) Syntheses, structural investigations, and ion-pairing phenomena of benzhydryltriarylphosphonium salts will be reported in a subsequent publication.
(43) (a) Mendes, P. *Comput. Appl. Biosci.* **1993**, *9*, 563−571. (b) Mendes, P. *Trends Biochem. Sci.* **1997**, *22*, 361−363. (c) Mendes, P.; Kell, D. B. *Bioinformatics* **1998**, *14*, 669−883. (d) Further information about Gepasi: www.gepasi.org.
(44) Alfassi, Z. B.; Neta, P.; Beaver, B. *J. Phys. Chem. A* **1997**, *101*, 2153−2158.
(45) Fingerhut, B. P.; Sailer, C. F.; Ammer, J.; Riedle, E.; de Vivie-Riedle, R. *J. Phys. Chem. A* **2012**, DOI: 10.1021/jp300986t.
(46) Exclusive formation of $\mathbf{E8}^+$ is observed after irradiation of **E8**-$PPh_3^+BF_4^-$ in CH_3CN; the plot for this system is shown in Figure S6 in the Supporting Information of ref 16.
(47) (a) Nakamura, M.; Miki, M.; Majima, T. *J. Chem. Soc., Perkin Trans. 2* **2000**, 1447−1452. (b) Tojo, S.; Yasui, S.; Fujitsuka, M.; Majima, T. *J. Org. Chem.* **2006**, *71*, 8227−8232.
(48) Fukuzumi, S.; Shimoosako, K.; Suenobu, T.; Watanabe, Y. *J. Am. Chem. Soc.* **2003**, *125*, 9074−9082.
(49) Griffin, C. E.; Kaufman, M. L. *Tetrahedron Lett.* **1965**, *12*, 773−775.
(50) Both groups have derived their conclusions from product studies after extended irradiation of benzyl triphenylphosphonium salts. It should be noted that product studies do not necessarily give the same results as transient measurements. Multiple irradiation of the same starting material molecules in preparative photolyses will distort the product ratios if the geminate recombination of one or both types of photofragment pair is a relevant process. Further complications arise if the photoproducts (e.g., arylmethyl halides) can undergo subsequent photolysis reactions.
(51) The observed rate constant k_{obs} for formation of $\mathbf{E12}^\bullet$ is the sum of the rate constants for phosphoranyl radical dissociation and back electron transfer. The derivation of this relationship is analogous to the case of the carbocation dynamics in the geminate solvent cage, cf. section S5 in the Supporting Information.
(52) Schneider, R.; Mayr, H.; Plesch, P. H. *Ber. Bunsen-Ges.* **1987**, *91*, 1369−1374.
(53) The absorbance maximum of the short-lived (<300 ps) $[\mathbf{E}^+\ Cl^-]$ ion pairs is also blue-shifted compared to the free $\mathbf{E}^+$. The dependence of λ_{max} on the distance between $\mathbf{E}^+$ and Cl^- is investigated in detail in ref 4.
(54) Krossing, I.; Raabe, I. *Chem.—Eur. J.* **2004**, *10*, 5017−5030.
(55) For nucleophilicity parameters of common photo-nucleofuges such as halides, carboxylates, tertiary amines, pyridines, tertiary phosphines, and others, see ref 41c.
(56) Mayr, H.; Schneider, R.; Schade, C.; Bartl, J.; Bederke, R. *J. Am. Chem. Soc.* **1990**, *112*, 4446−4454.
(57) (a) Mayr, H.; Schneider, R.; Irrgang, B.; Schade, C. *J. Am. Chem. Soc.* **1990**, *112*, 4454−4459. (b) Hagen, G.; Mayr, H. *J. Am. Chem. Soc.* **1991**, *113*, 4954−4961. (c) Mayr, H.; Patz, M. *Macromol. Symp.* **1996**, *107*, 99−110. (d) Burfeindt, J.; Patz, M.; Müller, M.; Mayr, H. *J. Am. Chem. Soc.* **1998**, *120*, 3629−3634.
(58) (a) Mayr, H.; Basso, N.; Hagen, G. *J. Am. Chem. Soc.* **1992**, *114*, 3060−3066. (b) Mayr, H.; Lang, G.; Ofial, A. R. *J. Am. Chem. Soc.* **2002**, *124*, 4076−4083.